Addis Ababa University
College of Technology and Built Environment
School of Biomedical Engineering
School of Graduate Studies

Biomechanical and Finite Element Analysis of Compressive Forces on the Lumbar Spine During Lifting Task by Ethiopian Construction Laborers

By

Beya Mulugeta

In Partial Fulfillment of the Requirements for the Degree of Master of Science in Biomedical Engineering

Advisor: **Dawit Assefa Haile (PhD)**

Addis Ababa, Ethiopia

December 2025

Declaration

I, the undersigned, declare that this thesis and the work presented in it are my own and have been generated by me as the result of my own original research.

I confirm that:

- This work was done wholly or mainly while in candidature for a research degree at this University;
- Where any part of this thesis has previously been submitted for a degree or any other qualification at this University or any other institution, this has been clearly stated;
- Where I have quoted from the work of others, the source is always given. With the exception of such quotations, this thesis is entirely my own work;
- I have acknowledged all main sources of help;
- This work or any part of this work has not been published before submission.

Name: _____Beya Mulugeta_____

Signature: _____

Date: _____14/5/2026_____

This MSc. thesis has been submitted for examination with my approval as an advisor.

_____

Dawit Assefa Haile (PhD)

Addis Ababa University

School of Graduate Studies

Certificate of Examination

This is to certify that the thesis prepared by Beya Mulugeta entitled: **Biomechanical and Finite Element Analysis of Compressive Forces on the Lumbar Spine During Lifting Task by Ethiopian Construction Laborers** submitted in partial fulfillment of the requirements for Degree of Master of Science in Biomedical Engineering (Biomedical Rehabilitation) complies with the regulation of the University and meet the accepted standards with respect to originality and quality.

Signed by examining committee:

Examiner: _Dr. Habtamu Mamo____Signature: _____Date: _____

Examiner: _Dr. Andinet Kumella____Signature: _____Date: _____

Chairman: _Mr. Bemenet Zelalem___Signature: _____Date: _____

_____

Chief of department or Graduate Program Coordinator

Acknowledgment

First, I want to express my deep gratitude to Lord Jesus Christ for guiding me through challenging times and enabling me to complete this thesis successfully.

My heartfelt thanks go to my advisors Dr. Dawit Assefa Haile for his priceless advice and guidance.

I am also deeply thankful to Mr. Deepak Muraya from Indian Institute of Space Science and Technology for his incredible support during the course of my thesis work. My appreciation extend to Mr. Muliye Kibabew, the former post graduate coordinator at the School of Biomedical Engineering, for his cooperation to access computing room whenever I needed it for my simulation.

Finally, I would like to acknowledge Dr. Meseret N. Teferra from Flinders University, Australia for his valuable information and guidance with my paper.

Abstract

Lower back pain (LBP) is a prevalent issue, particularly in physically demanding occupations like construction work, where heavy lifting and poor ergonomic practices significantly increase injury risks. In 2020, an estimated 619 million people worldwide were affected by LBP, with projections signifying a rise to 843 million by 2050. The construction sector in Ethiopia reports a high incidence of work-related lower back pain, yet research quantifying this issue is scarce. The current study aims to assess the biomechanical impacts of different lifting techniques and weight combinations on the lumbar spine to identify key factors contributing to lower back pain among construction laborers. To achieve this, the study evaluated 210 scenarios involving various lifted weights (0 to 125kg), lw - length of moment arm from lifted weight (0 to 0.5 meters), and α - angle between the extensor muscle force with body weight and lifted load (0° to 90°) using finite element analysis (FEA). The methodology involved converting 2D CT scan images into a 3D model for precise simulation of spinal stress under different conditions followed by model validation and FEA. The results revealed a maximum compressive force of 1419.71N when lifting 125kg at a 0° angle with a 0.5m moment arm and minimum compressive force of 126.196N at 90° angle with zero moment arm were obtained. The Von Mises stress result also ranged from 17.44MPa to 542.2MPa, showing peak stress at 0° angle and minimum at 90°. Increased weight and longer moment arms significantly raised the stress, particularly affecting the facet joints of L3, L4 and L5 of lumbar spine with the anterior part of L5 lumbar spine exhibiting significant stress. Further analysis indicated that directional deformation results of current study ranged from 0.0000629m to 0.001033m, with higher deformation associated with heavier loads and lower lifting angles. Despite reduced stress at higher angles, improper lifting techniques still posed risks. This result indicates the importance of minimizing the distance between the body and the lifted weight, as well as maintaining proper lifting posture as essential strategies for reducing compressive load on the lumbar spine and preventing injures. This study also highlights that heavier loads and upright posture increase compressive force, particularly in the L4-L5 region, posing a higher risk of long-term injuries. To mitigate these risks, a proper lifting technique, ergonomic intervention and workplace safety protocols that reduce compressive stress on the lumbar spine should be implemented. Reducing manual lifting needs, incorporating mechanical aids, and scheduling rest breaks can mitigate the risks. These measures are crucial for alleviating lumbar spine stress and preventing long-term injuries, such as disc herniation.

Key words: Lower Back Pain, Construction Laborers, Weight, Finite Element Analysis

Table of Content

List of Figures

List of Tables

List of Abbreviation

ALL	Anterior Longitudinal Ligament
ANSYS	Analysis System
AIDS	Acquired Immunodeficiency Syndrome
CT	Computed Tomography
CAD	Computer-Aided Design
DICOM	Digital Imagining and Communication in Medicine
E	Youngs Modulus
FEA	Finite Element Analysis
FEM	Finite Element Modeling
G	Shear Modulus
HIV	Human Immunodeficiency Virus
ITL	Intertransverse Ligament
IGES	Initial Graphics Exchange Specification
ILL	Iliolumbar Ligament
IVD	Intervertebral Disc
K	Bulk Modulus
LBP	Lower Back Pain
LF	Liagmentum Flavum
PLL	Posterior Longitudinal Ligament
SSL	Supra Spinous Ligament
STL	Stereo Lithography
TASH	Tikur Anbessa Specialized Hospital
2D	Two-Dimension
3D	Three-Dimension
V	Poisson Ratio

Chapter One
Introduction

1.1 Background

Lower back pain (LBP) is a widespread condition that affects a significant portion of the global population, leading to substantial disability and economic burdens [1]. This condition, which primarily affects the lumbar spine, is a prevalent musculoskeletal disorder among professionals engaged in physically demanding jobs, including drivers, carpenters, nurses, agricultural workers, welders and notably construction laborers [2]. As of 2020, an estimated 619 million people worldwide were affected by LBP, with projections indicating that this number could rise to over 843 million by 2050 [1].

In Africa, the annual prevalence of LBP is around 57%, although this issue is often overshadowed by other pressing health concerns such as malaria and HIV/AIDS. Limited healthcare access and poor workplace ergonomics worsen LBP, leading to reduced productivity at work [3]. The systematic review and meta-analysis of studies conducted in Ethiopia indicated that the annual prevalence of LBP is 54.05% [4].

Occupational health, defined as the highest degree of physical, mental and social well-being of workers across all occupations, is often compromised by work-related back pains [5]. The construction industry, recognized as one of the most hazardous occupations concerning workers safety and health, presents a particularly high risk for developing LBP due to the manual handling of materials such as carrying, lifting, lowering, pushing and pulling [6].

Historically, the incidence of LBP in construction workers has seen a gradual increase due to the rising demands and intensity of physical labor. The economic impacts of LBP are profound, including direct costs such as medical expenses and indirect costs like lost productivity and long-term disability, which collectively burden both individuals and industries [7]. Furthermore, LBP prevalence among construction worker is 50% higher than in other professions, with studies revealing that 71% of construction workers experience work- related LBP. Contributing factors include heavy lifting, awkward postures during lifting and prolonged physical exertion [8].

Advancements in biomechanical modeling and ergonomic assessment techniques, such as finite element analysis (FEA), offer new opportunity to better understand and address LBP. FEA allows detailed simulation of spinal stress under various lifting conditions, providing insights that can enhance ergonomic practices and safety measures [9].

In Ethiopia, the construction sector is the second- largest employer with over 1.8 million people, yet it also has one of the highest rates of work-related injuries [10]. A study conducted at Gonder University identified the leading causes of occupational injuries among Ethiopian construction workers as falls from ground level, overexertion during lifting and falls from elevation. Additional

factors such as aging, gender, job dissatisfaction, lack of vocational training and work overload further increase the likelihood of injuries [11].

This research addresses a critical gap in understanding work-related lower back pain among construction laborers, particularly in Ethiopia. Despite the high incidence of LBP in this sector, there is limited research that quantifies the biomechanical factors contributing to the problem. By providing a detailed biomechanical analysis, the findings can inform the development of ergonomic interventions and training programs aimed at reducing the risk of injury. Furthermore, this study contributes to the broader field of biomedical engineering by applying advanced modeling techniques to real-world occupational health issues. In this context, the current study aims to analyze the impact of compressive forces on the lower back with a specific focus on the lumbar spine during lifting activities performed by construction laborers using FEA. This analysis will consider variables such as the weight of carried load, the distance of lifting from the body and the angle between the extensor muscle force with body weight and lifted load. The findings from this study are expected to provide valuable insights for ergonomists in establishing safe lifting practices within the construction industry.

1.2 Lower Back Pain

LBP typically manifests in the lumbosacral region and can vary in severity, presenting as acute, sub-acute or chronic pain. Acute pain lasts up to four weeks, sub-acute between 4 weeks and 3 months, and chronic pain persists beyond 3 months. Treatments range from non-surgical options like physical therapy and medication to surgical interventions such as spinal fusion and intervertebral disc implantation [12].

LBP can arise from various factors including mechanical stress, injury and degenerative changes in the spine. When subjected to excessive loads or improper lifting techniques, the lumbar spine can experience significant stress, leading to pain and dysfunction. This underscores the importance of studying the biomechanical aspects of the lumbar spine to identify risk factors associated with LBP [13].

The current study focuses on understanding the biomechanical factors contributing to LBP in construction laborers, particularly the impact of compressive forces on the lumbar spine during lifting tasks. By analyzing these factors, the research aims to inform the development of ergonomic interventions that could reduce the incidence and severity of LBP in this high-risk group, aligning with the broader goal of occupational health.

1.3 Problem Statement

In countries like Ethiopia, where construction projects are booming, the incidence of LBP among workers is expected to rise. The surge in infrastructure development of roads, buildings, industries and health facilities has led to a significant increase in construction laborers. However, there is inadequate knowledge about how varying lifting conditions affects the lumbar spine.

Despite the high incidence of LBP among construction laborer, comprehensive studies analyzing specific biomechanical factors contributing to this condition are lacking. Existing literature often addresses general risk factors but fail to explore the detailed mechanics of spinal loading during occupational tasks. This gap hinders the development of targeted intervention to reduce LBP in this vulnerable population.

The impact of LBP ranges from limiting routine activities to causing serve injuries that could lead to disabilities or even death. Given current trends, LBP could become a major occupational health issue, imposing a significant societal burden. The current study aims to address this knowledge gap by conducting a rigorous biomechanical analysis of the lumbar spine under various loading conditions. By examining how different parameters affect spinal loading during lifting tasks, the research will provide valuable data to inform the development of targeted occupational lifting guidelines, enhancing worker safety in the construction industry.

1.4 Objective

1.4.1 General Objective

To analyze the impact of compressive forces on the lumbar spine under various lifting conditions by a construction laborer to develop a recommendation for safe lifting practices.

1.4.2 Specific Objectives

- ✓ To calculate compressive forces on the lumbar spine during various lifting setups.
- ✓ To develop a finite element model of the lumbar spine.
- ✓ To conduct a mesh convergence study to determine the optimal mesh size.
- ✓ To simulate different lifting scenarios using the developed finite element model.
- ✓ To assess the impact of load weight and lifting technique on spinal stress.
- ✓ To provide recommendations for safe lifting practices based on the findings.

1.5 Significance of the Thesis

This research holds significant importance in its contribution to understanding the biomechanical impact of lifting tasks on the lumbar spine, particularly in the context of construction laborers who are at high risk for developing lower back pain. It provides valuable insights into how attributes such as angle of force application, weight of object and moment arm length influence compressive forces and stress distribution in the lumbar spine. These findings not only enhance the current body of knowledge in biomechanics and occupational health but also have practical implications for reducing workplace injuries.

The study highlights the importance of proper lifting techniques and ergonomic interventions, which can inform the development of more effective workplace safety guidelines and training programs. By addressing a critical gap in the understanding of lower back pain risk factors among construction laborers, the study aims to improve worker safety, reduce injury rates and contribute

to the broader field of spinal health research. This result could also shape future policy and practices aimed at minimizing the incidence of lower back pain in high-risk professionals.

1.6 Scope and Delimitation of Study

This research mainly focuses on examining the biomechanical impacts of compressive forces on the lumbar spine during lifting tasks, specifically targeting the lifting practices of construction laborers. Using FEA, the research focuses on how different lifting conditions such as weight of the lifted object, moment arm length and compressive force angle, influence spinal stress and deformation. The study is limited to a short-term analysis of static load scenarios and does not explore dynamic lifting techniques or the cumulative effects of repeated lifting over time. Additionally, the study does not account for individual (different age, health condition, gender, etc) variability in the spinal response to different type of loads. Despite these boundaries, the research provides important perceptions into the biomechanical challenges of lifting, laying the groundwork for future studies on more complex loading conditions and long-term health impacts in labor-intensive environments.

1.7 Organization of Thesis

This rest of the thesis has been organized into four chapters. Chapter two includes an overview of the lumbar spine anatomy, biomechanics involved during lifting tasks and a review of studies using FEA to examine the effect of loading on the lumbar spine. Chapter three details the methodology, including the biomechanical analysis, finite element modeling, model validation and FEA simulation. Chapter four summarizes the core results of finite element analysis accompanied by some useful discussions. Finally, chapter five summarizes the research findings and offers recommendations for future studies.

Chapter Two
Literature Review

2.1 Lumbar Spine Anatomy

Good understanding of the anatomical components of the lumbar spine is fundamental for addressing lower back pains, which often arises from biomechanical stress. In adulthood, the vertebral column or spine consists of twenty-six bones: twenty-four vertebrae, along with a fused sacrum and coccyx. As illustrated in Fig. 1, these twenty-four vertebrae are organized into four regions: cervical, thoracic, lumbar and sacrococcygeal. The cervical and lumbar regions exhibit a concave curve, while the thoracic and sacrococcygeal regions form a convex curve. Together, these curves create the spine's S-shaped structure, functioning like a spring coil to maintain balance, absorb shock and allow a range of motion. Additionally, the spine plays a critical role in load transfer throughout the body, protects the spinal cord and facilitates mobility. Its design acts as a mechanical link between the upper and lower body, ensuring stable movement while protecting the spinal cord from injury [14].

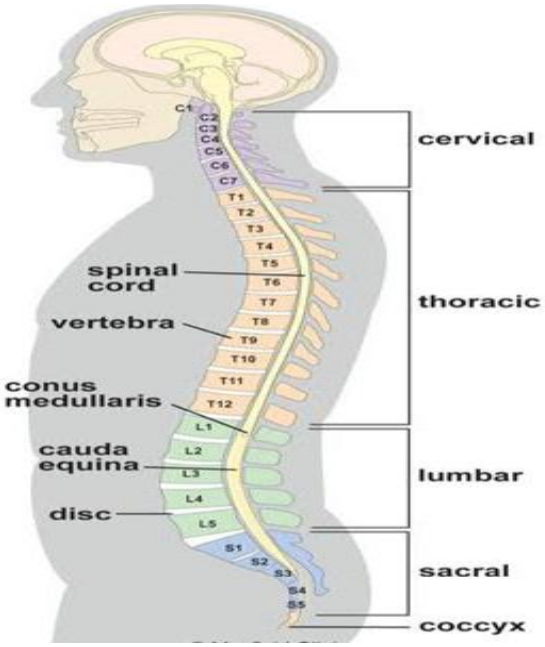

Figure 1: Cervical, thoracic, lumbar and sacrococcygeal vertebrae [15].

The lumbar spine, commonly known as the lower back, is the weight bearing section of the spinal column. It is composed of five vertebrae, labeled L1 to L5, along with intervertebral discs, ligaments and muscles. This part of the spine has a concave shape known as a lordosis curve, with the anterior portion being thicker than posterior. Each vertebra in the lumbar region has a cylindrical shape, measuring 30-35mm in depth and 40-45mm in width. These vertebrae consist of two types of bones: trabecular and cortical. Trabecular bone is a porous inner structure of the vertebra mainly

involved in red blood cell formation. The cortical bone is a dense outer layer of vertebra, which provides structural support [16].

In addition to their structural characteristics, the lumbar vertebrae have several anatomical features that support the spine's weight bearing function and mobility. As shown in Fig. 2, these include the spinous process, transverse process, pedicles, lamina, facet joint, mammillary process and vertebral canal. The transverse, mammillary and spinous processes serve as an attachment point for the muscle, contributing to the spinal movement and stability. The lamina links the transverse and spinous process while the pedicle connects vertebral body to the transverses process. The facet joint, located at the junction of lamina and pedicle, facilitate articulation between adjacent vertebrae allowing for controlled movement. Finally, the vertebral canal, a hollow passage within vertebra, protects the spinal cord from damage and allows blood vessels to pass through the central region of the intervertebral discs (IVD) [16].

The IVD is also a vital part of lumbar spine, located between the two vertebrae. It functions as a shock absorber and transfer the load between the adjacent vertebras. The IVD consists two main parts: the annulus fibrosus and the nucleus pulposus. The annulus fibrosus is a multi-layer collagen structure that enclose the nucleus pulposus and bears greater portion of the load applied. The nucleus pulposus is a gelatinous core responsible for evenly distributing the load [17].

Ligaments are also essential part of the lumbar spine, acting as connective tissues that link one vertebral body to another. Key ligaments in the lumbar region include the anterior longitudinal ligament (ALL), posterior longitudinal ligament (PLL), intertransverse ligament (ITL), supraspinous ligament (SSL), iliolumbar ligament (ILL) and Liagmentum flavum (LF). These ligaments play a critical role in maintaining spinal stability and restricting excessive movement [15].

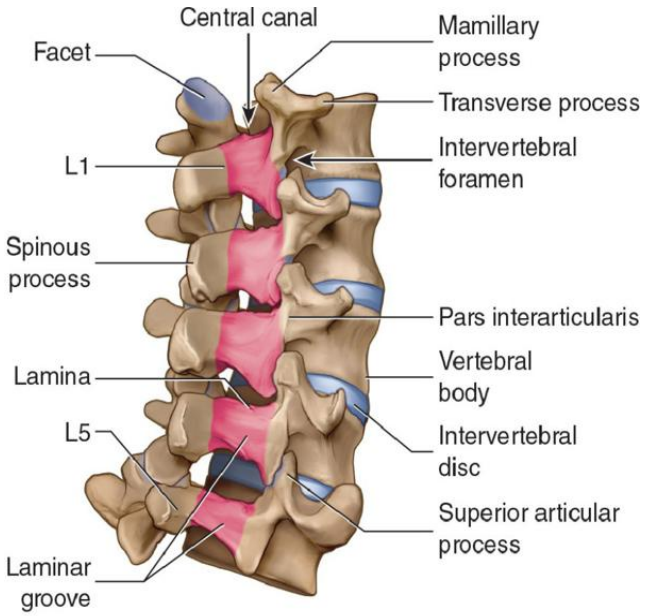

Figure2: Lumbar Spine [18].

2.2 Lumbar Spine Biomechanics While Lifting

During manual lifting, the lumbar spine involves managing compressive and shear forces that affect spinal health.To protect the spine, it is necessary to keep the lumbar lordosis while the core muscles stabilize and evenly distribute the body weight. Safe object lifting involves bending of the hip and not the waist. When bending to safely lift an object, the hip moves backward while the spine remains in a neutral, straight position. This movement engages the gluteal and hamstring muscles that are located on the lower body, minimizing the stress on the spine. Increased flexing movement of the spine will increase the shear forces on the lumbar vertebrae and intervertebral discs increasing the risk of injury. As seen in figure 3, during the lifting phase, the load is transmitted through the shoulder, upper back and core muscle to the lumbar spine. The spinal muscles involve increasing intra-abdominal pressure acting as an internal brace to reduce compressive forces and protect the spine from injury. Despite these protective mechanisms, the lumbar spine still exhibits significant compressive force. The risk of injury to the lumbar spine during this phase depends on several factors, including the body posture, weight of the load, frequency of loading, required force to relocate item and distance of moving item [19].

Figure 3: Force transmission during lifting [19].

2.3 Impact of Lifting on Lumbar Spine Biomechanics

Hambil et al. (2013) examined the impacts of manual lifting on the lumbar spine using finite element analysis with MSC Patran software. They developed a 3D model based on a scanning data to assess the stress and displacement change during lifting loads ranging from 20 to 60Kg. Their findings indicated significant stress variations with different lifting positions, particularly at fifth lumbar vertebra. Maximum stress ranged from 2.53MPa for lighter loads to 74.1MPa for heavier ones. The study emphasized the need for ergonomic interventions to prevent lower back pain (LBP) but had limitations in considering the variability in lifting techniques [20].

The other study conducted by Toda and Yamaoto (2016) developed a device to alleviate lower back pain during heavy lifting. Their device, featuring a three-point pad system, was tested at different angles with a 100N load. The device reduced rotational torque from 49Nm to 2Nm. This study underscores the importance of assistive devices but lacks consideration of real- world variability in lifting techniques and body types [21].

Siti Nurfaezah Zahari et al. (2017) studied the effect of physiological loading on the intradiscal pressure in the L1 and L2 of the lumbar spine. In the study, loads of 500N, 800N and 1200N were applied, representing a normal weight, overweight and obesity. Findings showed pressure increase with the load, particularly during flexion. The study highlighted the impact of physical loading but did not explore variations in demographic factors or preexisting conditions [22].

Xiang et al. (2021) investigated the biomechanical factors influencing peak compressive force (CF) during patient transfer tasks, a common cause of the lower back pain in the caregivers. Using a biomechanical simulator, variables such as trunk flexion angle, angular velocity and horizontal distance were measured between the wrist and lumbar region. The study found that peak compressive force typically occurs at the onset of lifting and is significantly impacted by trunk angular velocity and wrist-lumbar distance. The findings emphasized the importance of effective motion strategies to reduce lower back pain risks during patient transfer tasks. This study did not explore the effects of diverse loading scenarios, particularly in other work settings [23].

Han et al. (2021) investigated spinal loads during manual lifting tasks by developing a 3D biomechanical model. Using data from CT scans, electromyography (EMG), and a motion analysis system, the effects of lifting various loads (0N, 90N and 180N) on the lumbar spine was assessed. The study found maximum external flexion moments at L3-L4 disc compression force ranging from 469.5N to 601.5N. Dynamic lifting tasks resulted in increased disc compression forces compared to static lifting, with variation between 15.8 % and 39.4 %. Additionally, erector spinae muscles contributed about 40% of the total muscle force during lifting. The findings highlight the importance of understanding spinal loads to develop preventive strategies against lower back pains, though further research is needed to refine the model and explore effects of additional variables [24].

Zhang et al. (2024) used FEA to explore the effects of symmetric bending and lifting in a weightlifter with L4- L5 disc herniation. Their study found uneven stress distribution, with maximum stress at the anterior inferior margin of L5 lumbar spine. The research highlights the importance of understanding spinal biomechanics in individuals with lumbar disorders but does not account for different lifting patterns or load distributions [25].

The study in the current thesis aims to address gaps identified in previous research by examining the effects of lifting loads on spinal units in the case of construction laborers. It will incorporate diverse lifting conditions to provide a comprehensive analysis of their effect on the spinal stress. The findings will offer a detailed understanding of how different lifting conditions affects the spinal stress, thereby enhancing the development of more effective solution and strategies to prevent lower back pains.

Chapter Three
Methodology

3.1 Biomechanical Analysis

In this section, a detailed biomechanical analysis was conducted to evaluate the compressive forces acting on the lumbar spine during lifting tasks commonly performed by construction laborers. The analysis aims to understand how factors such as angle between the extensor muscle force with body weight and lifted load (α), lifted weight (W), and Length of moment arm from lifted weight (lw) influence the forces exerted on the lumbar spine. A series of biomechanical equations were applied across 210 different loading scenarios to quantify the impact of these variables on the spinal loading. The results from these calculations are then applied to a 3D model of the lumbar spine for FEA, allowing for a comprehensive examination of how these forces affect the spine's structure under various loading conditions.

3.1.1 Participants

A hypothetical model representing a young, healthy construction laborer with an ideal body weight of 53Kg is used in the biomechanical analysis. This weight is chosen based on general health guidelines and reflects typical body weight standard for individual in this demographic [26]. The model serves as a baseline for evaluating compressive loading and stress of lumbar spine under various lifting conditions, providing a standardized reference point for analyzing the biomechanical effects of different lifting scenarios.

3.1.2 Force Analysis

The biomechanical calculations are carried out to determine the erector spinae muscle force (F_{muscle}), total axial compressive force ($F_{vertbare}$) and the specific axial compressive force on the L1 lumbar spine (F_{L1}). The analysis included 210 different loading scenarios, which were evaluated to compare the impact of different lifting conditions on lumbar spine loading, and to identify scenarios with the highest risk of injury.

As illustrated in the Fig. 4, a combined anatomical and mechanical view of the lumbar spine under a lifting condition, presenting how different force interact to maintain equilibrium. The upper body weight (Fbw) and lifted load (Fwl) act downward, creating a forward bending moment on the lumbar spine. The erector muscle force (Fmuscle) counteracts the moment created from both upper body weight and lifted load. In addition, the diagram highlights the impact of moment arms and angle of muscle action to the magnitude of force, which contribute to stress concentration in lumbar spine.

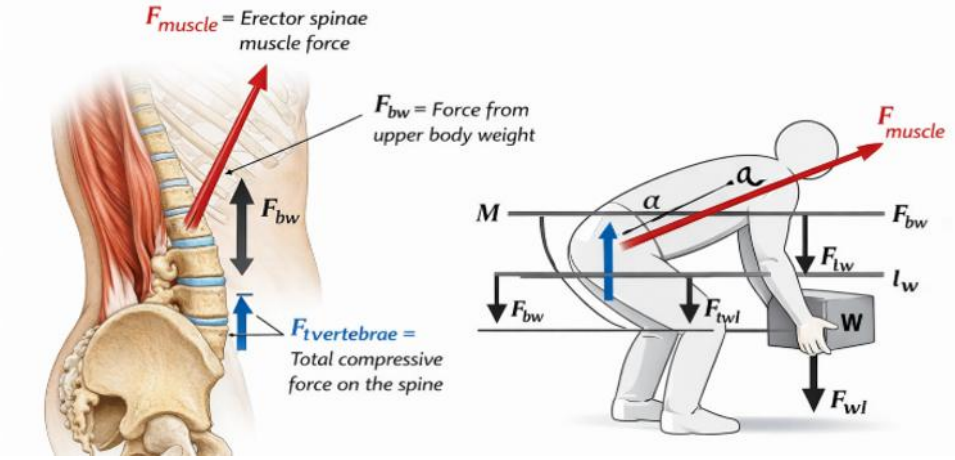

Figure 4: Anatomical and Biomechanical diagram of lumbar spine loading during lifting

Free Body Diagram

As seen in Fig. 5, a free body diagram is developed to illustrate the force acting on the lumbar spine during lifting tasks. This includes the Erector spinae muscle force (F_{muscle}), the force from the upper body weight (F_{bw}) and the force from the lifted weight (F_{wl}). The erector muscle force represents the stabilizing support provided by the erector spinae muscles as they contract. The force from the upper body weight reflects the pressure exerted on the lumbar spine by the weight of the upper body. Finally, the force from lifted weight denotes the additional load applied by the object being lifted [30].

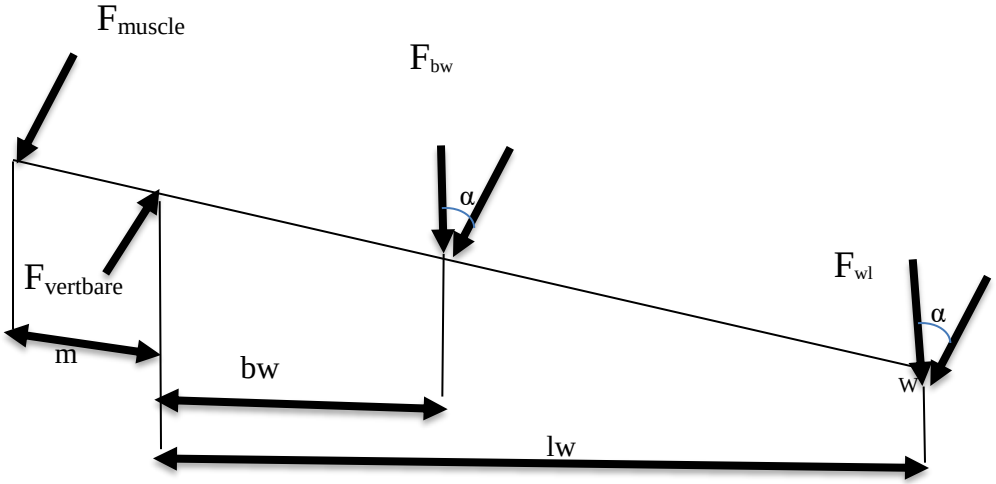

Figure 5: Free body Diagram for the Force acting on the lumbar Spine.

where, F_{muscle} = Erector spinae muscle force, F_{bw} = Force from upper body weight, F_{wl} = Force from lifted weight, $F_{vertbare}$ = Total compressive force on the spine, M = Length of moment arm from Erector spinae muscle, bw = Length of moment arm from center of gravity of the body weight, lw = Length of moment arm from lifted weight, α = Angle between the extensor muscle force with body weight and lifted load, W = Lifted Weight.

Variables Considered

Key variables in the analysis include:

- Based on findings from previous studies, the calculation of compressive forces applied on the lumbar spine uses 65% of the total body weight to represent the upper body weight [27].
- Construction laborers frequently handle various materials such as sacks, concrete, stillage and machinery. As shown in Tab. 1, the list of these materials along with their respective weights is taken as a reference. For the current study, the weights used in the analysis were {0, 15, 25, 50, 75, 100 and 125 kg} to reflect the range of loads typically lifted in the construction work.

Material type	**Unit**	**Average Weight (Kg**
Cement	Bag	50Kg [28]
Sand	Cub/ft	20Kg/safest 15Kg [29]
Aggregate	Cub/ft	60 -70Kg [29]

Table1: Construction material types and their Weights.

- Length of moment arm from erector spinae muscle (m) was set at 0.06 meters. This value aligns with findings from Mc Gills (1997), who extensively studied the biomechanics and the length of moment arm was in the range of 5 cm to 6 cm. Keeping this value constant allows for consistent basis for comparing muscle forces and their effects on the lumbar spine under different lifting conditions [31].
- Length of the moment arm from the center of gravity of body weight was set at 0.254 meters. This parameter is based on biomechanical model presented by McGill (1997), who analyzed the lumbar spine loading during lifting tasks. McGill's work indicates that the center of gravity for the upper body is approximately at this distance [31].
- Length of moment arm from lifted weight (lw) was varied from 0.0 to 0.5 meters - {0.0, 0.1, 0.2, 0.3, 0.4, 0.5}. This range is chosen to reflect different lifting techniques, from holding on object close to the body to lifting it farther away. Hambali Ariff et al. (2013) demonstrated that increasing the distance of the load from the body significantly affects lumbar spine torque and compressive forces [20].
- Angle variation between the extensor muscle force with body weight and lifted load (α) is assumed to be between 0° and 90° - {0°, 30°, 45°, 60°, 90°}. The selected angle variation represents different body postures during lifting. Analyzing 0° to 90° allows this study to explore a broad spectrum of lifting postures, consistent with real world conditions, and their corresponding impacts on the lumbar spine forces.

Procedure

The compressive forces on the lumbar spine were calculated using the equations below, accounting for moment arms, object mass and lifting angles. A total of 210 loading conditions were analyzed, varying the load position, lifting angle and object mass.

At equilibrium, summation of all moments should be zero, i.e. ∑M = 0. This implies:

$$F_{muscle} * m - F_{bw} * bw - F_{wl} * lw = 0 \Rightarrow F_{muscle} = \frac{F_{bw} * bw + F_{wl} * lw}{m} \quad (1)$$

Again, at equilibrium, summation of all forces should be zero, i.e. ∑ F=0. This gives rise to:

$$F_{vertbrae} - F_{muscle} - F_{bw} * Cos\ \alpha - F_{wl} * Cos\ \alpha = 0 \quad (2)$$

Combining Equations (2) and (3) and combining it with Equation (1) , we can derive the following:

$$F_{vertbare} = \frac{(F_{bw} * bw + F_{wl} * wl)}{m} + (F_{bw} * Cos\ \alpha + F_{wl} * Cos\ \alpha) \quad (3)$$

The above equation implies that the total load acting on the spine vertebrae is the sum of body weight, lifted weight and extensor muscle force. While from the total load on the spine, 11% of axial compressive load acts on the L1 of the lumbar spine [32].

3.2 Development of the Finite Element Model

3.2.1 Data Acquisition

A 64- slice CT scan machine at Tikur Anbessa Specialized Hospital (TASH) was used to obtain cross-sectional image. CT scans captured from a 25-year-old healthy male were used in this study to develop the finite element model. The age of the subject (25 years) was chosen based on typical reference standards for healthy adult demographic which ensure the model's relevance to common clinical and research scenarios.

3.2.2 Segmentation

The Mimcs21.0 software was used for this process which provided advanced modeling features and compatibility with multiple operating systems [33]. It was employed to reconstruct the gray scale 2D images into a 3D model of the lumbar spine. Intensity values ranging from 226 to 2976 were utilized to distinguish bone structure from other tissues, while values between -700 and 225 were used for segmenting the intervertebral discs. These threshold values were automatically determined by Mimics software. The segmented lumbar spine was then extracted using the segment editor tool, resulting in a non-manifold assembly of the lumbar spine. The final 3D geometry file of the lumbar spine was obtained in stereo lithography (STL) format using 3-Matic software, which is included in the Mimics software package. Figure 6 (a) and (b) shows the snapshots of the 3D segmented vertebral body and intervertebral disc.

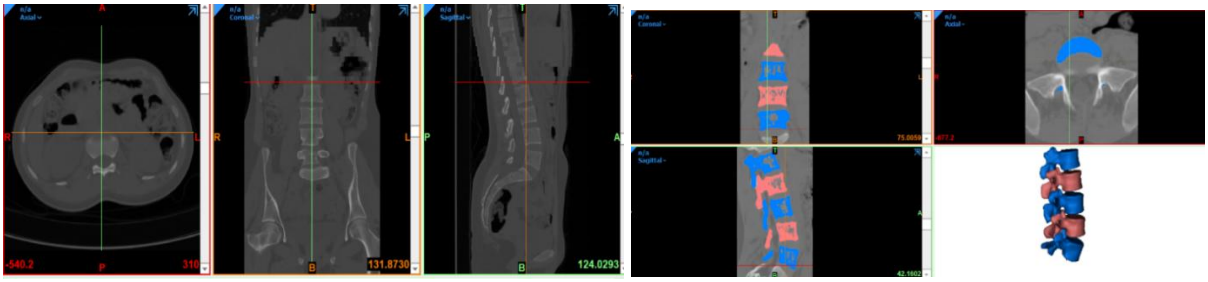

(a)

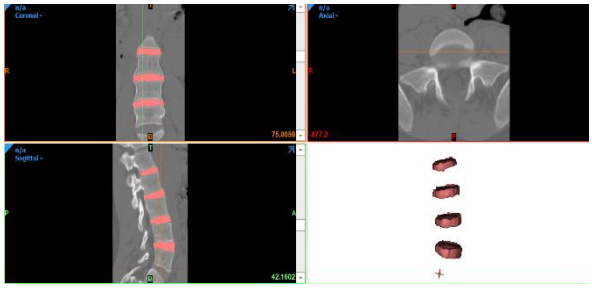

(b)

Figure 6: (a) Segmentation of L1-L5 Lumbar vertebrae, (b) Segmentation of L1-L5 intervertebral disc.

3.2.3 Finite Element Model Construction

The STL file from Mimics 21.0 was imported into Geomagic Design X software for further processing. This software converted the STL file into a high-end Computer-Aided Design (CAD) file in Initial Graphics Exchange Specification (IGES) format. The Auto surface tool in Geomagic Design X was used to fit a surface patch mesh and create the surface body. A local 3D contour of the STL file was extracted to build a network surface patch over the lumbar spine geometry. Any intersecting pairs, poor patch angles or high deviation patches were then corrected to ensure an optimal 3D CAD file. Finally, before exporting the whole model, a smoothing factors of 0.5 was applied to create smooth surface for 3D geometry of the lumbar spine without distorting the original structure. As shown in Fig. 7(a) the final model on the lumbar spine was taken out in IGES format for further analysis. Similarly, the STL file for Intervertebral Disc (IVD), generated by Mimics 21.0 software was also converted into CAD file using Geomagic software. The IVD was then segmented into two components: the annulus fibrosus and the nucleus pulposus. Based on previous studies, 40 - 55% of the IVD was assigned to the nucleus pulposus, while the remaining portion was designated as the annulus fibrosus [16]. Figure 7(b) shows the finite element model of the intervertebral disc, illustrating these components. The output from this process was saved in IGES file format for use in the next step.

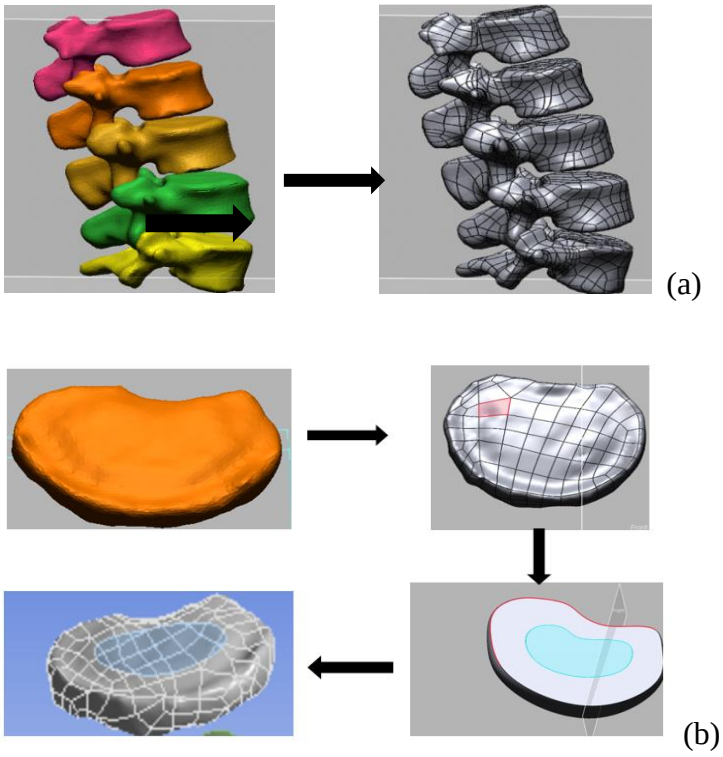

Figure 7: A 3D model construction for (a) vertebrae and (b) Intervertebral disc.

Following the previous step, the IGES file was imported to Analysis System (ANSYS 19.0) Space Claim software where an offset of 0.5mm was applied on each vertebra to represent the cortical bone. The remaining bone was modeled as cancellous bone, in accordance with previous literature [34]. This offset helps to differentiate between the dense cortical bone and spongy cancellous bone in the finite element model. Figure 8 illustrates the final finite element model, highlighting the distinct layers of cortical and cancellous bones.

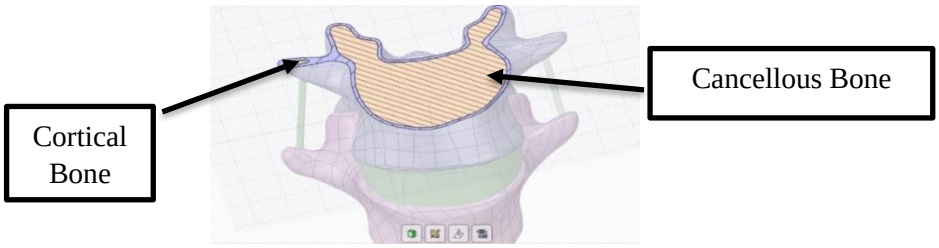

Figure 8: Modeling of cortical and cancellous bone.

The modeling of spinal ligament including the inter transverse, supra spinous and inter spinous ligament was carried out using ANSYS 19.0 software. Table 2 provides the dimension of these ligaments used in the modeling that was taken from previous studies. Following the modeling of the ligaments, final model assembly, which included vertebrae, intervertebral discs and ligaments, was completed using ANSYS 19.0 software. The comprehensive assembly is shown in Fig. 9 providing a visual representation of integrated model used for subsequent analysis.

Ligament	Cross Sectional Area (mm^2)	Reference
SSL (Supraspinous ligament)	35	[16]
ISL (Interspinous ligament)	8	
ITL (Intertransverse ligament)	35.5	

Table 2: Dimension of the ligament for FEM.

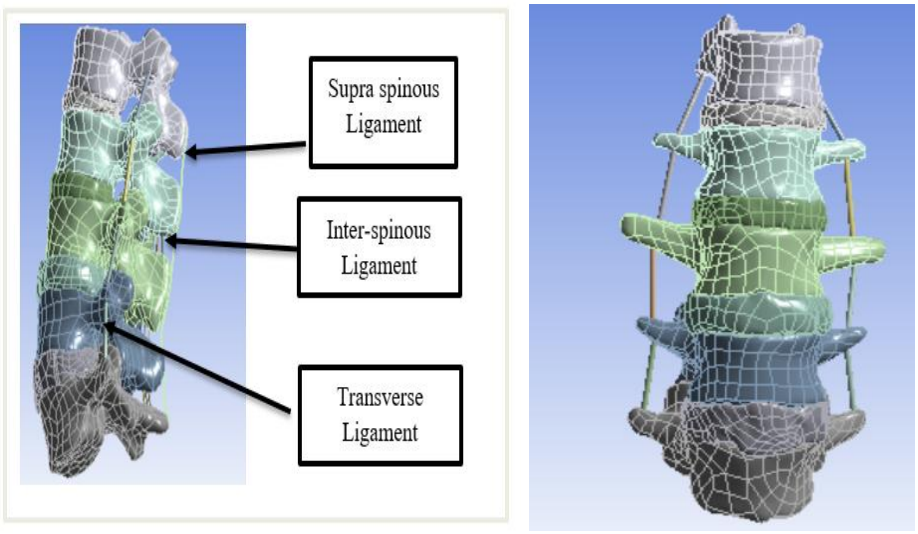

Figure 9: Finite element modeling of ligament and the final FEM.

3.3 Material Properties

The material properties used in the analysis were carefully derived from previous studies. The vertebral body was represented as a linear, isotropic material, while viscoelastic properties were assumed for the annulus fibrosus and nucleus pluposus. A viscoelastic property was assigned for the annulus fibrosus and nucleus pluposus in order to simulate its response under loading conditions. The ligaments were modeled as linear elastic, tension only elements to represent their characteristic behavior effectively. Table 3 provides a summary of the material properties utilized in the current study.

			Properties			
No	**Part**	**Material**	**Youngs Modulus E (MPa)**	**Poisson Ratio V (μ)**		**Reference**
1	Cortical bone	Linear, Isotropic elastic	12000	0.3		[35]
2	Cancellous bone	Linear Isotropic elastic	100	0.3		[35]

3	Inter-spinous Ligament	Linear Elastic Tension only element	10	0.3		[36]
4	Inter-transverse Ligament		10	0.3		
5	Supra-spinous Ligament		8	0.3		
6	Annulus fibrosis	Viscoelastic matrix nonlinear elastic fiber	8	0.45		[36]
	Annulus fibrosus prony Series coefficient					
			Time (sec)	**Bulk modulus (K)**	**Shear Modulus (G)**	
			3.45	0.399	0.399	
			100	0.3	0	
			1000	0.149	0.361	
			5000	0.150	0.108	
7	Nucleus pulpous	Viscoelastic solid	2	0.45		[36]
	Nucleus pulpous prony Series coefficient					
			Time(sec)	**Bulk modulus (K)**	**Shear Modulus (G)**	
			0.141	0	0.638	
			2.21	0	0.156	
			39.9	0	0.120	
			266	0	0.0383	
			500	0	0	

Table 3: Material properties.

3.4 Mesh Convergence Study

To ensure the finite element model's accuracy and reliability, a mesh convergence study is conducted. This involves systematically refining the mesh size and analyzing the resulting changes in Von Mises stress outputs. The goal is to identify a mesh size that provides stable and constant results, ensuring the model accuracy predicts the lumbar spine's biomechanical responses. In addition, this study provides input for selecting mesh element size of the FEA to obtain an accurate result with a moderate computing time.

As indicated in Table 4, the mesh element size ranges from 1 to 100 milli meter representing conditions from fine to coarse mesh resolutions. For the analysis, an axial rotation moment of 7.5Nm was applied. An axial rotation is the most sensitive movement to a mesh resolution [37]. For loading conditions, the bottom of the L5 vertebral body was fixed and quadratic tetrahedral

mesh is applied. The resulting maximum Von Mises stress is computed for each mesh scenario using ANSYS 19.0 software.

Mesh Scenario	Mesh Element Size (mm)	Element Number	Node Number
Mesh 1	1	494741	911870
Mesh 2	2	194969	368444
Mesh 3	3	128373	245096
Mesh 4	4	109459	210880
Mesh 5	5	102317	198340
Mesh 6	6	97054	188688
Mesh 7	7	93480	181862
Mesh 8	8	89369	174010
Mesh 9	9	86911	169369
Mesh 10	10	85849	167329
Mesh 11	20	85071	165712
Mesh 12	30	85049	165710
Mesh 13	70	63520	140721
Mesh 14	100	60342	139321

Table 4: Mesh convergence scenarios and its respective Element size.

3.5 Loading and Boundary Condition of the Study

A pure compressive force was applied to the L1 lumbar spine with varying magnitudes to simulate the 210 loading scenarios. The boundary conditions for simulation involved fixing the lower end of the L5 lumbar spine, thereby establishing a stable base while applying the compressive load to L1 vertebra. These conditions are illustrated on Fig. 10, which provides a visual representation of applied force and constraints.

For the FEA, a quadratic tetrahedral mesh with a given element size (considering the 14 mesh scenarios) was employed to capture the detailed geometry of spinal structures. A linear bonded contact condition was used to model the interactions between different components of the spinal model. All the finite element analysis in the current study was conducted using ANSYS 19.0 software.

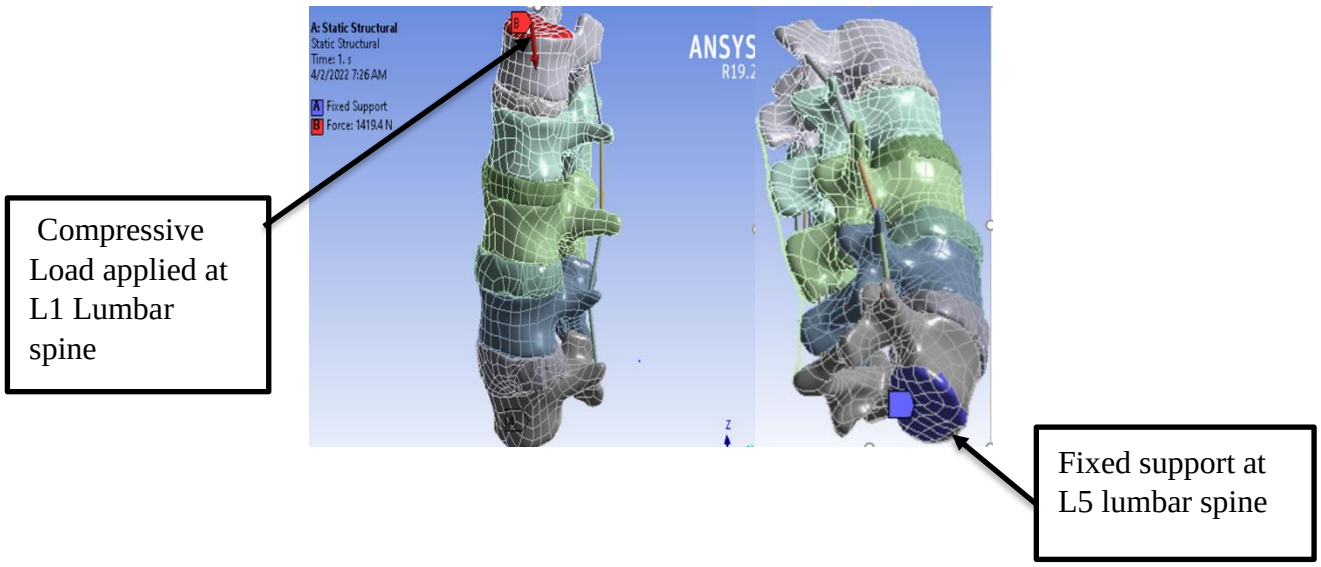

Figure 10: Boundary Condition: Compressive Load at L1 and fixed support at L5 lumbar spine.

Chapter Four
Results and Discussion

4.1 Overview

This section presents the findings of the biomechanical analysis and FEA conducted to evaluate the impact of compressive forces on the lumbar spine during lifting tasks performed by a construction laborer. The analysis explores how various factors such as weight of the lifted object, angle of force application and length of moment arm affect the stress and deformation experienced by the lumbar spine. The research aimed to quantify the stress on the lumbar spine under different lifting conditions and identify which biomechanical factors contribute significantly to the risk of lower back injuries. The findings are discussed in the context of implication towards workplace safety and development of recommendation for safe lifting practice to reduce the incidence of lower back pain among construction laborers.

4.2 Biomechanical Analysis of Lumbar Spine under Compressive Loading

In the current study, compressive forces on the lumbar spine were calculated based on the principle of equilibrium and biomechanical analysis. The calculation incorporated key variables such as lifted weight (W), angle between the extensor muscle force with body weight and lifted load (α), and length of moment arm from lifted weight (lw) across 210 distinct loading scenarios. The analysis calculated the extensor muscle force needed to maintain lumbar spine equilibrium by balancing moments from body weight and lifted object weight. The total compressive forces on the spine were obtained including contribution of the extensor muscle force, lifted object weight and body weight with particular focus on the compressive load experienced by the Lumbar vertebras.

The results presented in Appendix I reveal a relationship between the force exerted by the erector spinae muscles (F_{muscle}) and the total compressive load on the spine. The study indicates that as the lifted weight and length of moment arm increase, the force required from erector spinae muscle also rises resulting in a higher total compressive load on the spine. A significant portion of this load is concentrated on the lumbar spine highlighting its vulnerability to injury during heavy lifting tasks. This suggests the importance of minimizing the distance between the body and the lifted weight, as well as maintaining proper lifting posture as essential strategies for reducing compressive load on the lumbar spine and preventing injures.

Figures 11 and 12 illustrate the compressive force on the lumbar spine in relation to W, lw and α. The result indicates that the compressive load on the lumbar spine consistently increases with the lifted weight following a clear trend across the different moment arm lengths. Furthermore, the length of the moment arm plays a crucial role; as it increases from 0 to 0.5 meters, the compressive load on the lumbar spine escalates across all measured angles.

When α is 90°, the spine primarily experiences shear forces due to the horizontal alignment of erector spinae muscle force, with a reduced compressive force. This is because the body weight is perpendicular to the muscle force. Even though the compressive force at this angle is low, the near horizontal alignment of the erector spinae muscle and upper body weight increase the shear force that act parallel to the vertebrae which could also promote intervertebral disc shear and injury on the lower lumbar spine.

Conversely, when α is 0°, the body weight force is aligned with the erector spinae muscle force, leading to the highest compressive load on the lumbar spine, as both forces are acting in the same direction along the spine's axis. This increased load places stress on the intervertebral discs and vertebrae, leading to risks like disc degeneration and vertebral fractures. As the angle α decrease from 90° to 30°, the compressive force on the lumbar spine increases incrementally, as a greater component of the body weight force is aligned with the spine's vertical axis. This increase in compressive force alleviates pressure on the spine and reduce the risk of compressive-related injuries but it simultaneously increases the risk of shear-related injuries. The above results indicate that posture of the body during lifting activities plays a critical role in determining the amount of stress placed on the lumbar spine. The finding of this analysis highlight importance of using proper lifting technique and maintain good body posture during lifting to reduce injury risk, as both mechanics of lifting and the weight being lifted significantly influence the load on the lumbar spine.

Further investigating the graph in Figs. 11 and 12, the highest compressive load recorded is 1419.71 N, occurring when a worker lifts a 125kg load with angle (α) set at 0° and lw set at 0.5 meters. The compressive force on the lumbar spine is highest at 0° with both the body weight and lifted load acting to the spine vertically downwards, which lead highest load to act on the lumbar spine. Conversely, the minimum compressive load of 126.196 N is observed when the moment of the arm is zero (lw=0) and the angle (α) is set 90°. When moment arm length is set at zero (lw=0) and angle (α) is set at 90°, the compressive force on the lumbar spine remains constant across all lifted weights because the body weight force acts directly downward without contributing additional compressive stress.

In conclusion, to minimize the risk of lumbar spine injury while lifting, it is important to adopt a neutral spine position and bend at the hips and knees rather than waist. Maintaining an angle between 30° and 45° relative to the vertical axis to balance compressive and shear forces helps to evenly distribute the load and reduces strain on the lumbar spine. The analysis indicates that engaging core muscles keep the load close to the body and use legs for lifting are effective strategies. Additionally, avoiding the extreme angles (near 0° and 90°) is important as either these can increase the compressive or shear forces, respectively, thus raising the risk of injury.

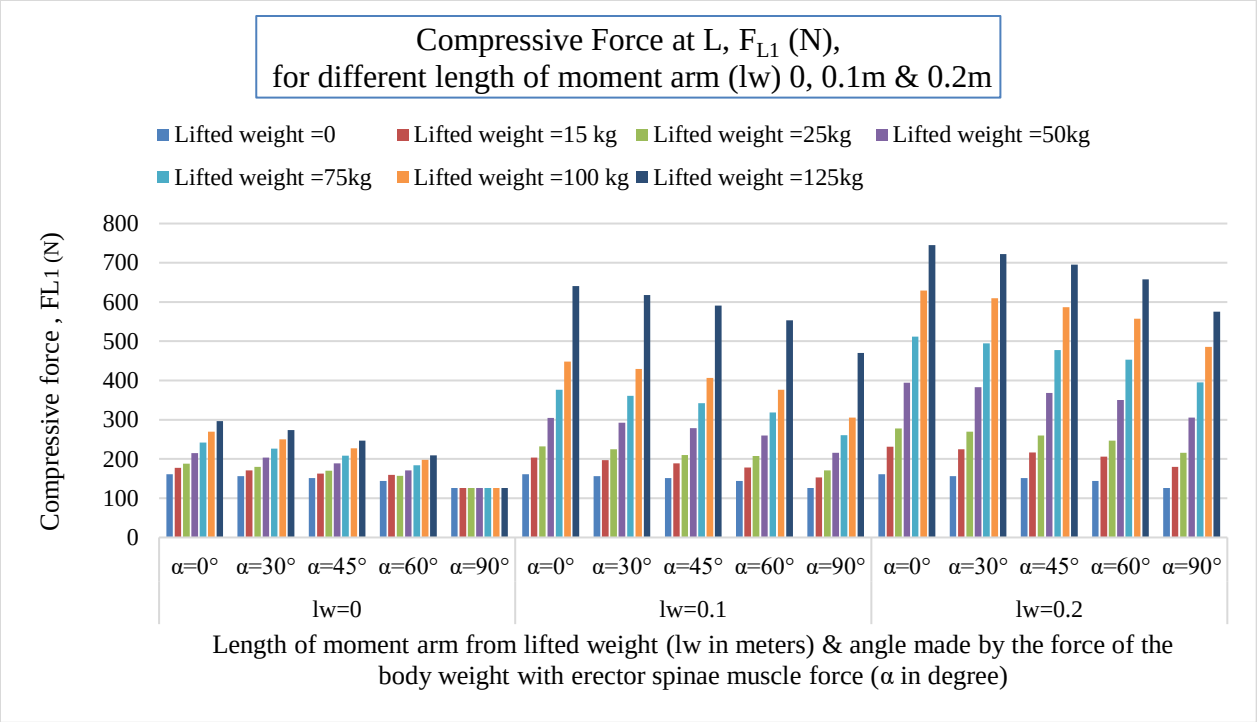

Figure 11: Compressive Force at L_1 (F_{L1}) vs. Length of moment arm (lw) set at 0, 0.1m & 0.2m.

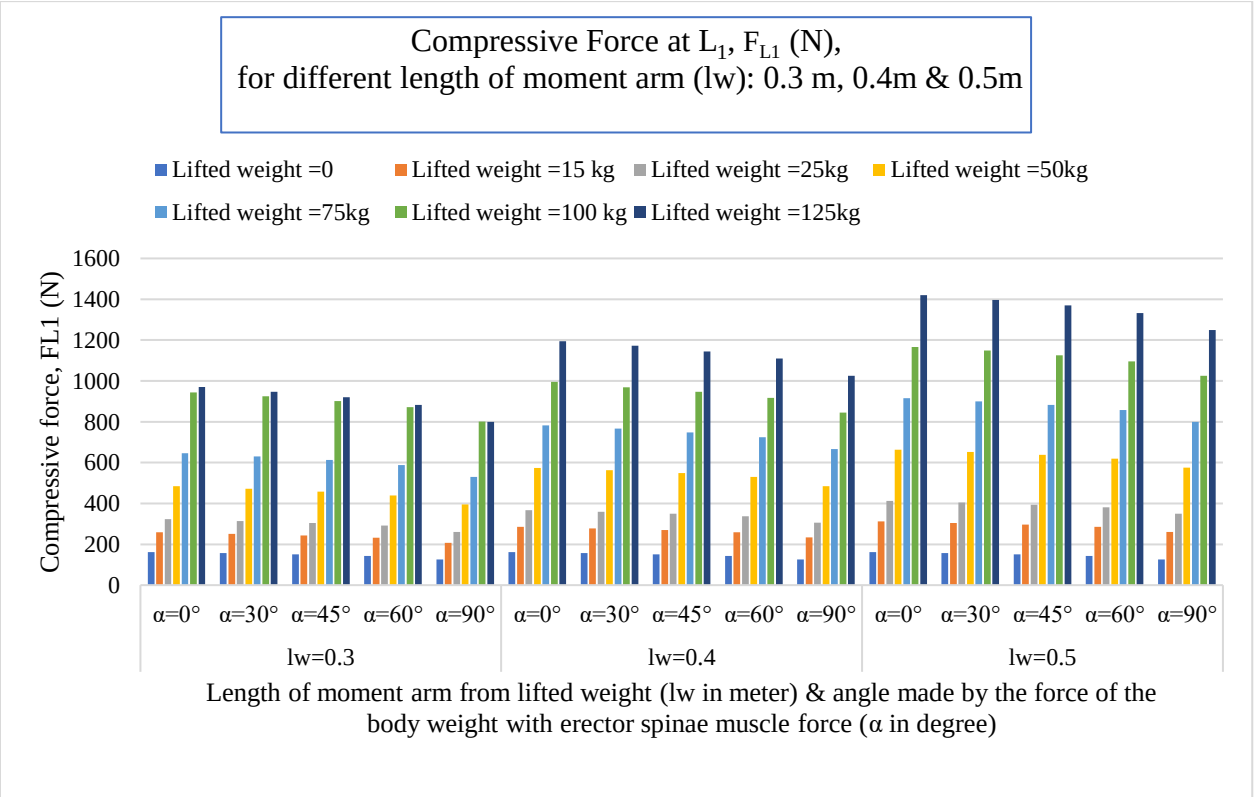

Figure 12: Compressive Force at L_1 (F_{L1}) vs Length of moment arm (lw) set at 0.3, 0.4m & 0.5m.

4.3 Mesh Convergence Study Result

In the current study, the mesh convergence test was performed to determine the optimal mesh size for accurately modeling the biomechanical behavior of the lumbar spine during lifting tasks. This step ensures that the simulation results, such as stress and deformation are reliable and independent of mesh density, there by validating the FEM used in this research. In the current study, as shown in appendix III, the mesh convergence test was conducted by applying fourteen different element sizes to the FEM ranging from fine to coarse meshes.

In a complex geometry such as lumbar spine, the mesh convergence is defined by monotonically with mesh refinement. The finer mesh may capture numerical stress singularities near load application region, resulting in exaggeratedly higher stress values. Therefore, mesh convergence was assessed by identifying a mesh independent plateau in stress response. The plot in Fig. 13 illustrates how varying the mesh element size affects the computed stress within the lumbar spine model. It shows that as the mesh element size decreases, the Von Mises stress value initially change significantly. However, after reaching a certain mesh size, the stress value stabilizes indicating the further refinement of the mesh does not lead to substantial change in the results.

As shown in Fig. 14, the test result indicated that Von Mises stress values stabilize around 37 MPa even though element size change. For element size of 7mm up to 20mm, the stress value stabilized approximately at 37.06 MPa, with variation below 1%. Therefore, the stress result converges in this scenario, meaning, FEM is reliable and further refinement would only increase computational cost with inaccuracy of the results.

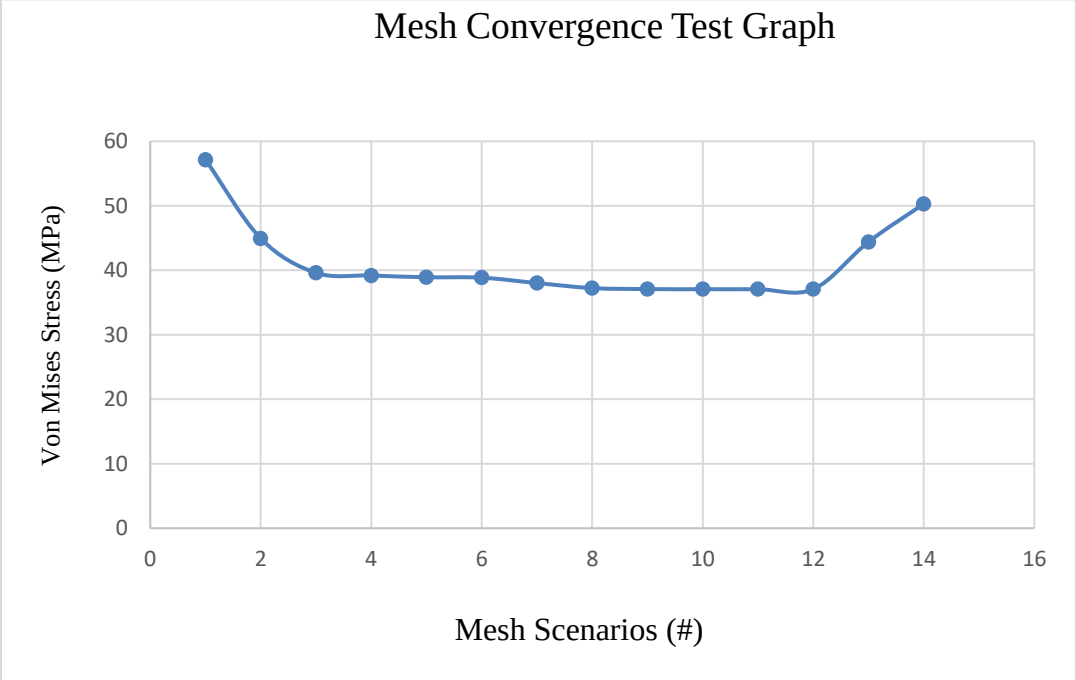

Figure 13: Mesh convergence test graph.

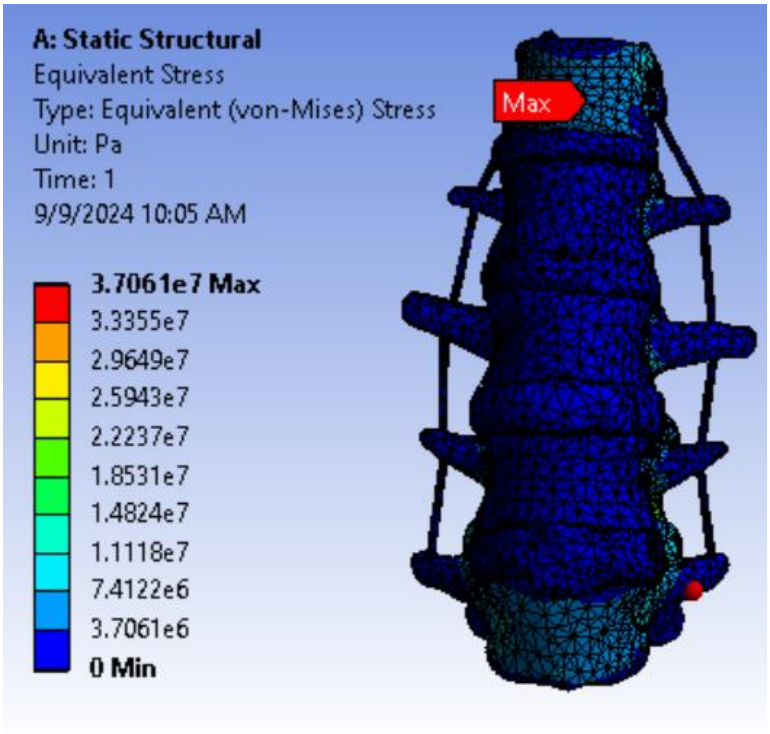

Figure 14: Von Mises stress result with element size at 0.01m.

4.4 Finite Element Analysis

4.4.1 Equivalent Von Mises Stress Result

In the current study, an equivalent Von Mises stress analysis was conducted to determine distribution of stress in the lumbar spine when subjected to various compressive forces arising from different lifting conditions. The table presented in Appendix II shows the resulting stress values for 210 corresponding lifting conditions. The analysis shows that the Von Mises stress value ranges from 17.44 MPa up to 542.2 MPa depending on the lifting weights varying from 0 kg to 125 Kg. The result demonstrates a clear linear correlation between increased lifting weight and Von Mises stress value, underscoring the lumbar spine vulnerability to injury as the lifted weight increases.

As noted in appendix II, increasing the length of moment arm (lw) from 0.1 to 0.5 meters, raises the compressive force applied to the lumbar spine, resulting in higher stress levels. This occurs because the body must exert counterforce to stabilize and lift the load. The effect is particularly noticeable when the angle (α) is set at 0°, as this combination of a longer moment arm and direct vertical loading increase stress. As shown in the Fig. 15, the maximum Von Mises stress value i.e. 542.2 MPa is obtained when length of moment arm is set to 0.5 meter. This indicates that when a worker lifts a weight away from the body, there is a higher likelihood of lower back pain or injury compared to lifting the weight closer to the body.

The analysis of the Von Mises stress distribution in the lumbar spine under different lifting angles provides important insight into the spinal biomechanics. The highest Von Mises stress occur at an

angle (α) of 0°, where the force of body weight aligns directly with the spine in an upright position. In this posture, the spine experiences significant compressive force because the entire load is transmitted vertically along the spinal axis, leading to higher concertation of stress in the lumbar region. Conversely, at angle (α) 90°, where the body is fully bent over, Von Mises stress is at lowest. Although the spine experience increased shear force due to the horizontal alignment of erector spinae muscle, direct compressive load on the spine is reduced. The bending posture distributes forces differently across the spine resulting in lower stress concertation compared to the upright position. As the angle (α) decreased from 90° to 30°, the rise in Von Mises stress due to compressive forces on the lumbar spine can have notable effects. This increased Von Mises stress can lead to significant strain on the lumbar spine, potentially causing disc degeneration, vertebral fractures, and other spinal injuries. The result highlights the importance of proper lifting angles to minimize adverse effects on the lumbar spine.

The bar charts in Fig. 15 and 16 also illustrated a valuable insight on the Von Mises stress distribution in relation to weight lifted, the angle between the extensor muscle force and the body (α) and the length of moment arm from lifted weight. The higher weights lifted correspond to greater Von Mises stress value particularly at longer moment arm lengths. The Von Mises stress remain relatively constant as no weight is lifted, regardless of change in the length of moment arm. This is because, absence of an external load. Only body weight and internal muscle forces are acting on the lumbar spine, which balance each other without generating additional stress. Consequently, with no weight being lifted, the length of the moment arms has a minimal influence on the resulting stress value. Other than the no weight case, for the other weightlifting scenarios, the maximum equivalent Von Mises stress value increase linearly with increase in moment arm from 0 to 0.5m.

In conclusion, minimizing the length of moment arm by keeping the load close to the body and reducing the weight of the load are recommended strategies for reducing lumbar spine stress. Lifting with the body in an upright position intensifies compressive stress while bending at a 90° angle reduces compressive stress but increases shear forces. These findings highlight the importance of optimizing lifting angles to effectively manage the stress and reduce risk of lumbar spine injuries.

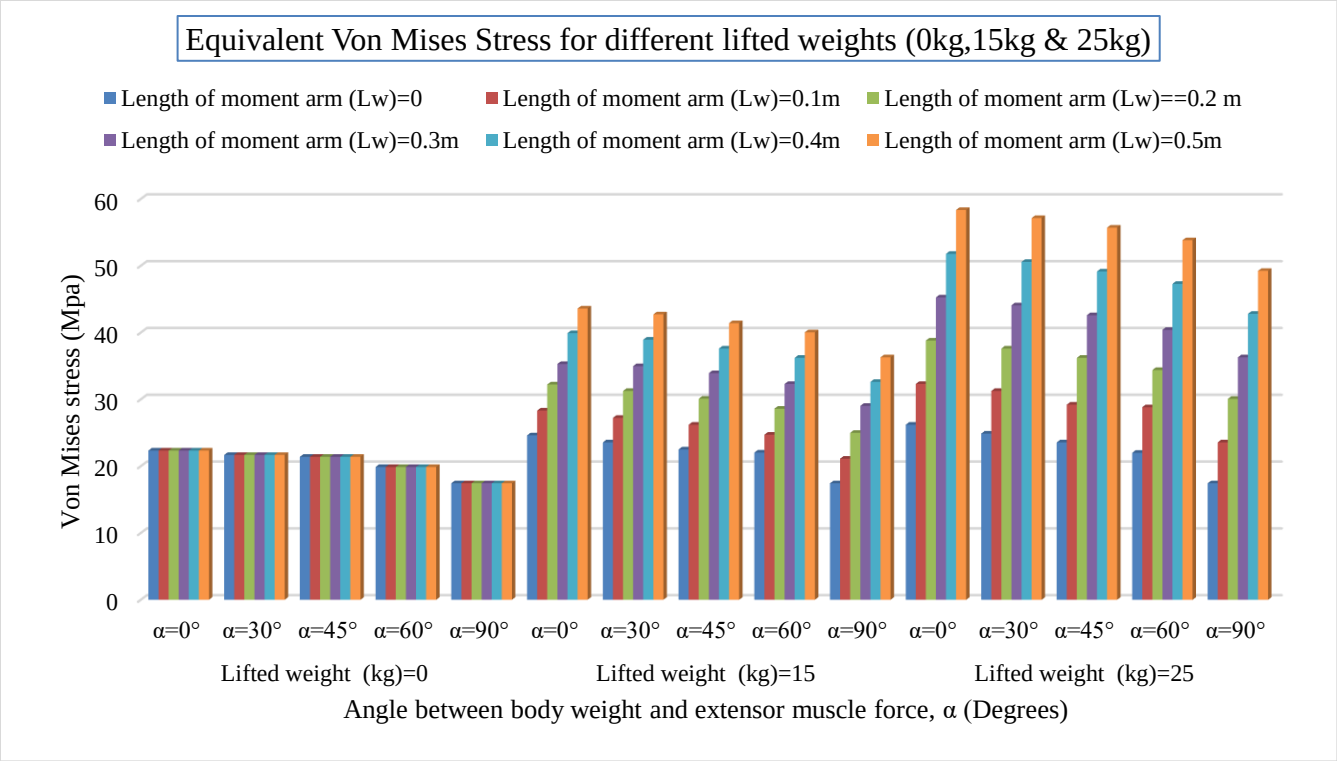

Figure 15: Equivalent Von Mises Stress Comparison for 0kg, 15kg & 25kg loads.

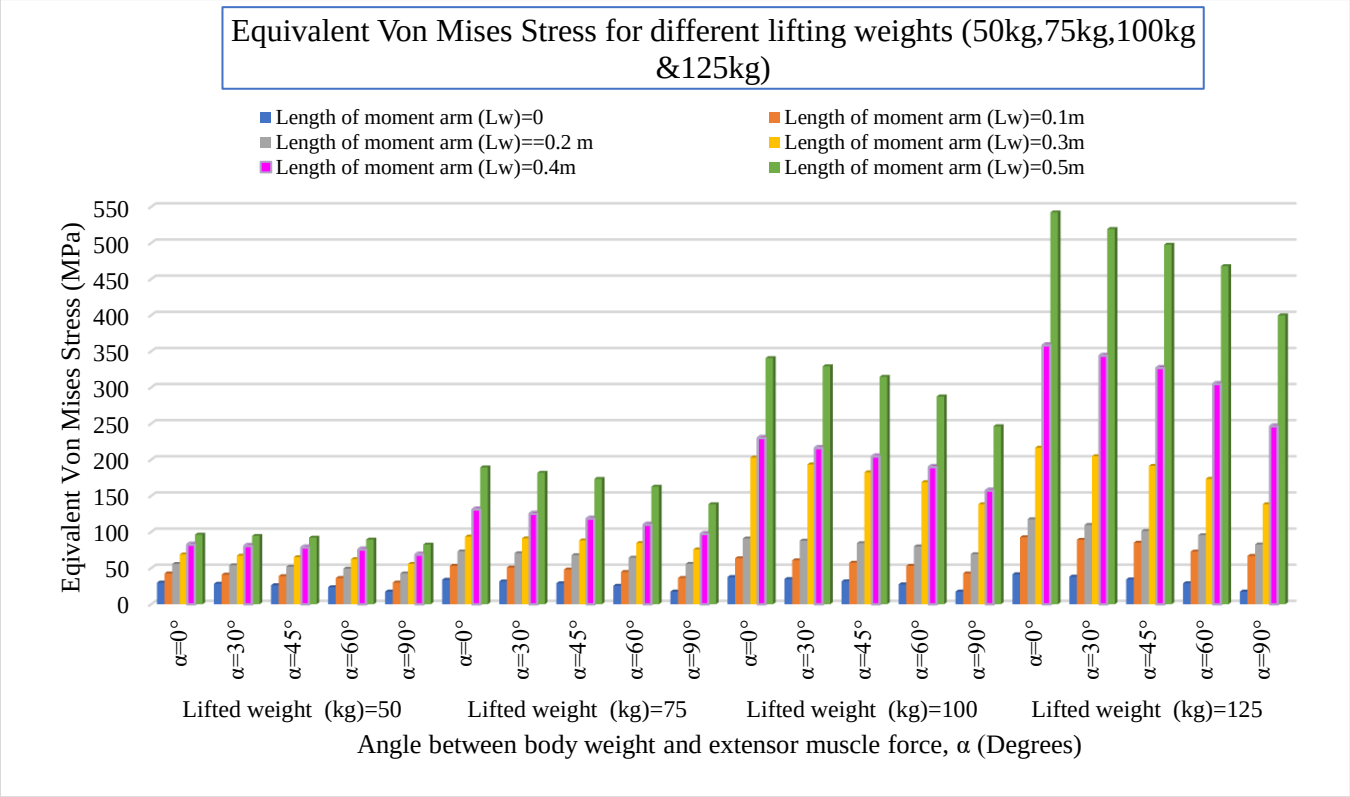

Figure 16: Equivalent Von Mises Stress Comparison for 50kg, 75kg, 100kg & 125kg loads.

The stress distribution trend in all loading conditions is similar, primarily concentrating within vertebral bodies, and with increasing the lifted weight, the stress value escalates. As illustrated in Fig. 17, significant distribution of the equivalent Von Mises stress was noted in the facet joints of L3, L4 and L5 vertebrae. This observation is crucial as facet joints play a significant role in stabilizing the spine and are key structures in managing compressive loads during lifting activities. The elevated stress in these joints highlights their vulnerability under increased compressive forces.

A stress concentration at L5 vertebra were also observed when lifting a heavy object. This shows an effect of weight lifting on increasing mechanical stress at the lower back. This finding is consistent with anatomical structure and function of the lumbar spine, where the lower vertebrae, especially L5 are positioned to support the majority of the body's weight during lifting tasks.

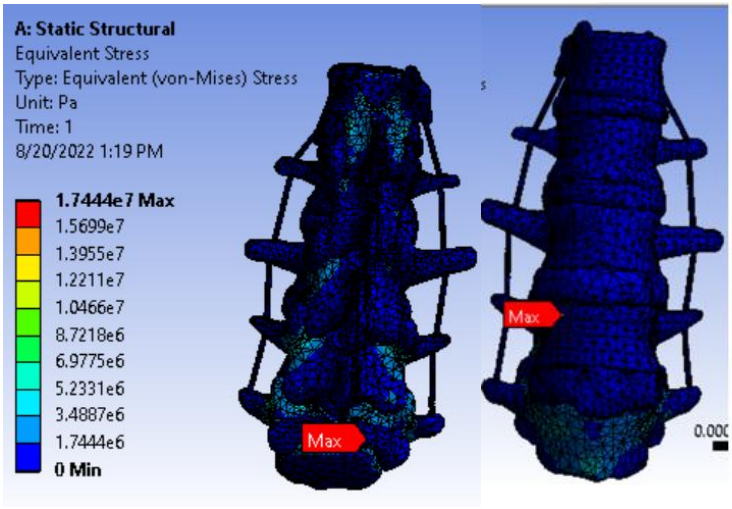

(a)

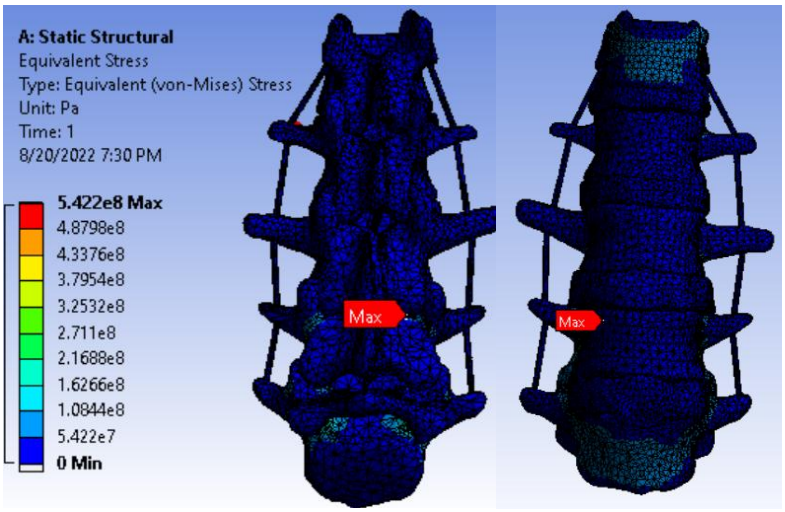

(b)

Figure 17: Von Mises stress distribution of the Lumbar Spine: (a) When lifted weight is zero, lw at zero and α= 90°; (b) When lifted weight is 125kg, lw at 0.5m and α=0°.

As seen in Fig. 18, a closer examination of the stress distrubtion in the lower three lumbar vertbrae reveals that the pedicle and facet joints experince a signficant amount of stress. With the increase in lifting weight, the magnitude of Von Mises stress in these area signficantly rises. This result highlights the fact that posterior elements of the spine, which play cruical role in stablizing and guiding spinal movement, are subjected to higher mechanical demands during lifiting activites.

Overall, the study underscores the potential for significant wear and tear on the lumbar spine, particularly in the facet joints and vertebral bodies, due to the compressive stresses experienced during lifting tasks. This finding emphasized the importance of focusing on these specific areas when developing preventive strategies and interventions to protect the lumbar spine from long-term damage. Proper lifting techniques and ergonomic practices are crucial in mitigating these risks and preserving spinal health.

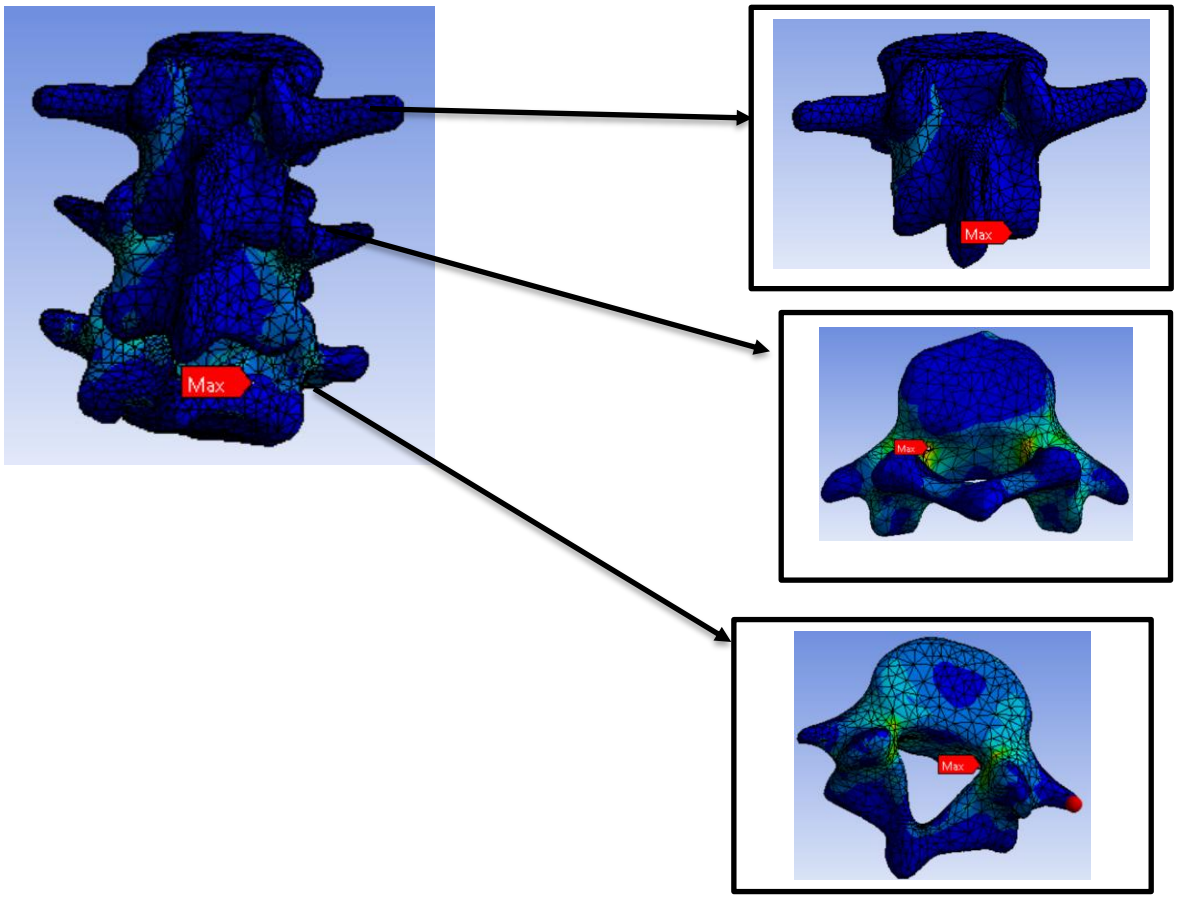

Figure 18: Von Mises stress distribution in L3-L5 Lumbar Spine.

4.4.2 Directional Deformation Result

Directional deformation describes how the lumbar spine displaces under the applied compressive force, indicating how the spine deforms under different loads (see Appendix II). This analysis is important for assessing the risk of injury due to excessive deformation. The study reveals that the direction deformation value ranges from 0.0000629m to 0.001033m. This indicates a significant

increase in deformation as the lifted weight goes from 0kg to 125 kg, which is critical in evaluating injury risk. This mechanical response of the lumbar spine to compressive force highlights the increased risk of injury as the weight being lifted approaches or exceeds physiological limits.

The length of moment arm (lw) plays a critical role in determining deformation of the lumbar spine. This moment arm (lw) increases the torque on the spine, leading to higher deformation on the lumbar vertebrae and intervertebral disc. As seen in Fig. 19, when the moment arm approaches zero, the deformation is smaller, but it rises sharply as the moment arm increase to 0.5 meters. At lower angle (α) ranging from 0° to 30°, where body is at upright posture, the compressive load acts directly along the lumbar spine, leading to significant deformation on the lumbar region. In contrast, when the body is bent forward at angle (α) between 45° to 90°, the compressive force on the lumbar spine is reduced, resulting in less deformation. However, the presence of shear forces during bending can still exacerbate lumbar spine deformation under certain conditions. Concisely, the result of the current study indicates that as the compressive forces were reduced at higher angles, improper lifting techniques in such posture may still cause significant stress on the spine.

.

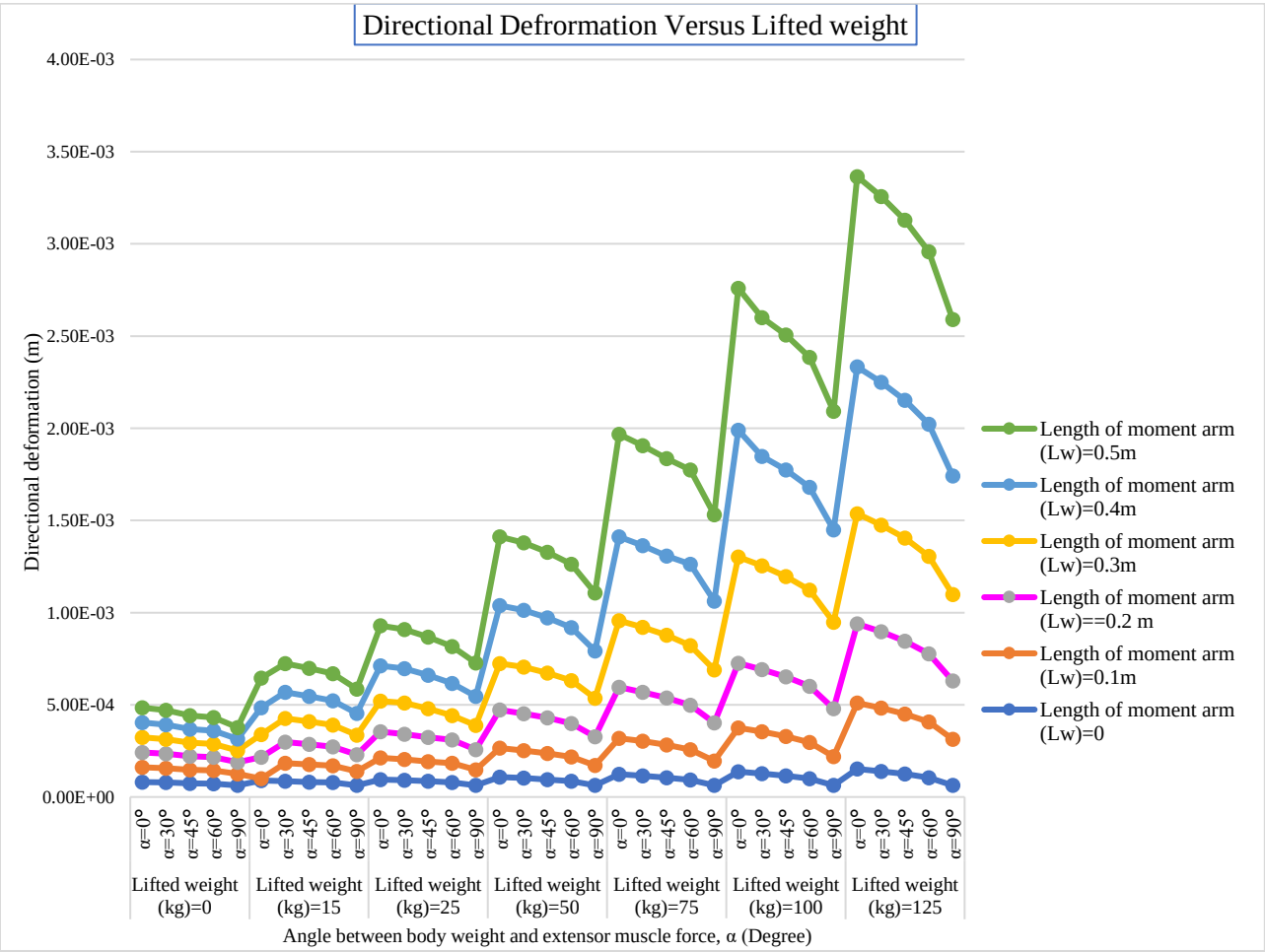

Figure 19: Directional deformation when length of moment arm (Lw) is set at: 0, 0.1, 0.2, 0.3, 0.4 & 0.5 meter.

As seen in Fig. 20, the deformation of the lumbar spine begins in the upper segments and intensifies as it moves downward, with L3, L4 and L5 exhibiting significant increase in a deformation. The results indicate that the lower lumbar vertebrae, specifically L3, L4 and L5 experience more significant deformation compared to the upper lumbar vertebrae. Although the deformation in L2 is less compared to lower lumbar region, L2 still exhibits some deformation. This pattern arises due to accumulation of stress and weight in the lower lumbar regions.

Notably the anterior portion of the vertebral body shows a higher degree of deformation compared to the other regions. The increase in deformation is primarily due to greater load distribution and biomechanical stress concertation in this area. Compressive forces during lifting or bending often place more stress on the anterior part of the vertebrae exacerbated by the viscoelastic nature of the intervertebral disc.

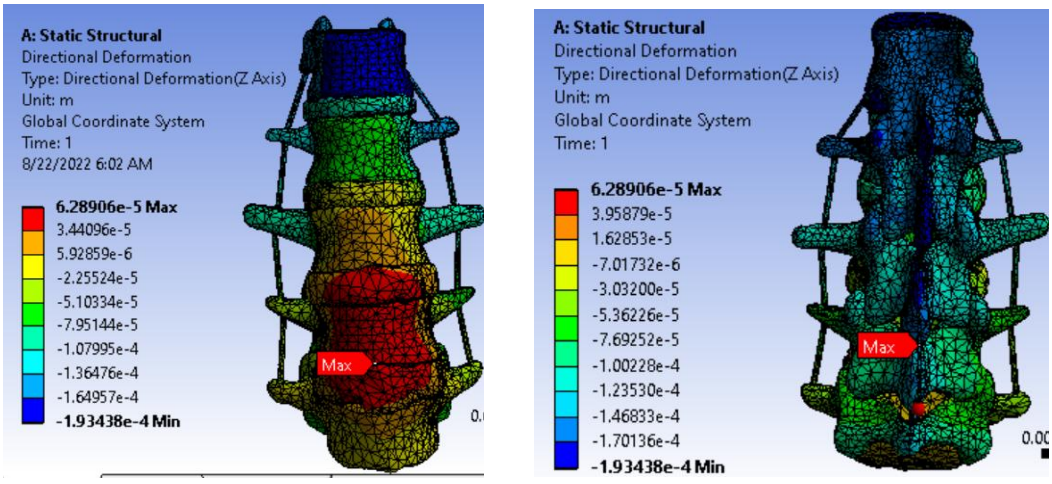

(a)

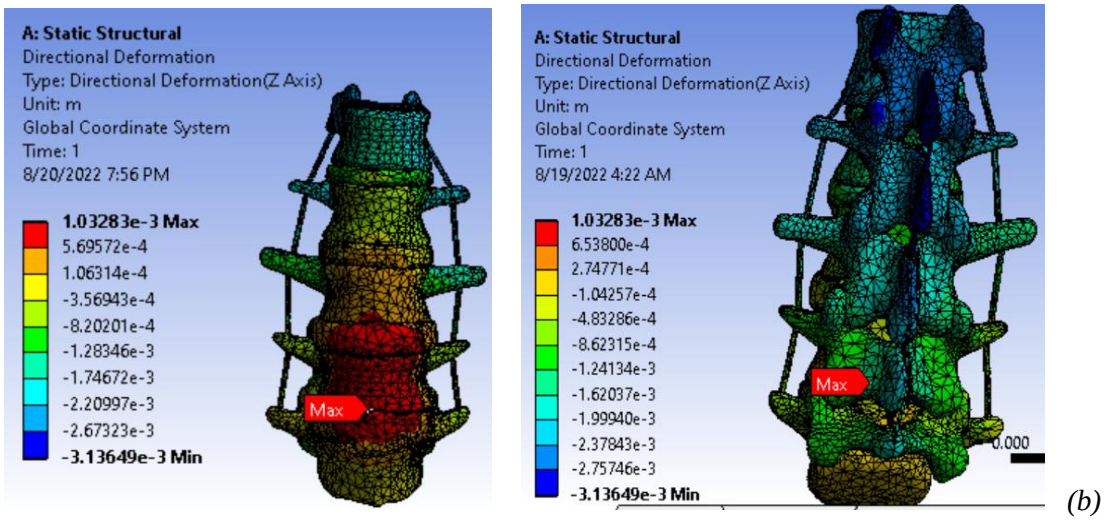

(b)

Figure 20: Directional deformation of the Lumbar Spine: (a) When lifted weight is zero, lw is zero, α= 90°; (b) When lifted weight is 125kg, lw is 0.5m, α=0°.

In the current study, when closely observing the directional deformation response of the lumbar spine, it becomes evident that deformation of the intervertebral disc increases progressively from L1 to L5, with the most significant deformation occurring at the L3-L4 and L4-L5 intervertebral discs. As shown in Fig. 21, the anterior part of the annulus fibrosus experiences a higher degree of directional deformation compared to the nucleus pulposus. Deformation begins at the outer edge of the annulus fibrosus and gradually extend inward, a result of the viscoelastic properties of the nucleus pulposus that allow it to distribute the applied load in various directions. These findings indicate that the lower lumbar spine (L3-L5) endures the most of compressive forces, making it more susceptible to injury and degeneration overtime.

In summary, a higher risk of disc related issue such as herniation might occur in the lower lumbar region. The reduced deformation in L1-L2 intervertebral disc indicates that this region is more resistant to compressive stress but the increased load bearing responsibility of the lower lumbar spine highlights the importance of focusing on this area in ergonomics and clinical interventions to prevent injury.

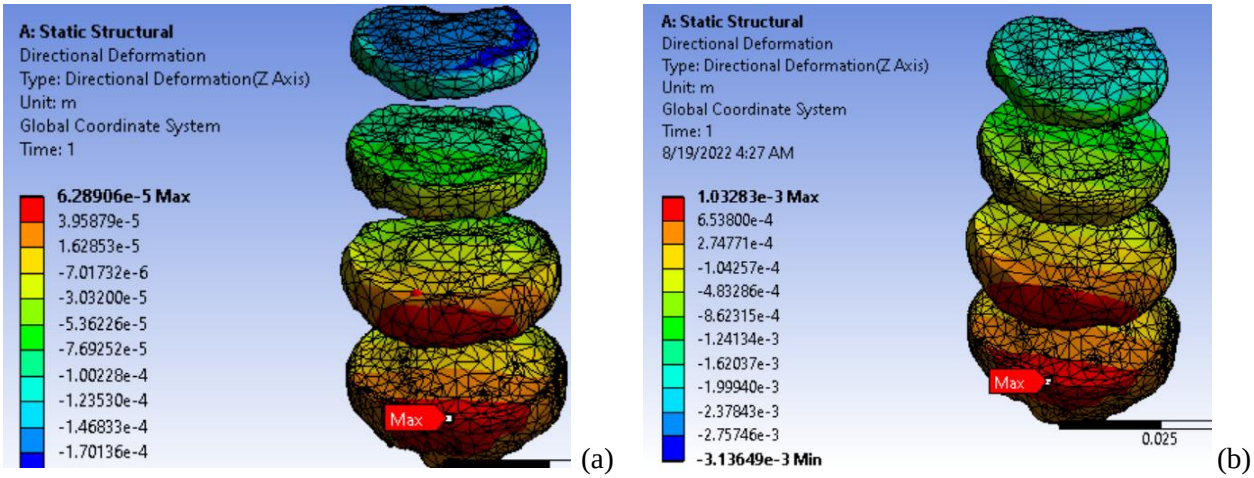

Figure 21: Directional deformation of the intervertebral disc Lumbar Spine: (a) When lw = 0, α=90° while lifted load is zero; (b) When lw at 0.5m, α=0° while lifted weight is 125kg.

4.5 Discussion

In the current study, the findings provide critical insight into the biomechanical response of the lumbar spine under various lifting conditions, particularly the compressive forces that influence spinal health during lifting tasks. The mesh convergence result, along with the analysis of lifting parameters such as weight of lifted object, moment arm length and body posture, offer a robust understanding of the factors that contribute to the lumbar spine stress and injury risk in physically demanding environments.

In the current study, based on the mesh convergence test, the Von Mises stress levels of at around 37 MPa with less than 1% variation across element size from 0.007m to 0.02m. Previous study on the lumbar spine by Shash and Eden (2025) reported that mesh convergence was obtained when successive Von Mises stress change remained within 5% change throughout refinements [38]. This

indicates that stabilizing stress responses through mesh refinement is important for biomechanical analysis.

The Von Mises stress values in the current study range from 17.44 MPa to 542.2 MPa across various lifting conditions, ranging from 0 to 125kg. Hambali Ariff et al. (2013) performed FEA on a lumbar spine model under manual lifting conditions, while loading ranged from 20 kg to 60 kg. Maximum Von Mises stress from this study ranged from 2.52 MPa to 74.1 MPa [20]. Although the absolute Von Mises stress values differ significantly, both studies indicated a consistent trend of increasing spinal stress with increasing lifting load. In addition, both studies show that increasing both the moment arm and lifting weight significantly elevates stress levels, reinforcing the importance of proper posture and load handling techniques.

The directional deformation values found in the current study, ranging from 0.0000629m (0.07mm) to 0.001033m (1.03mm), indicate alignment with established computational benchmarks for the lumbar spine. A study conducted by Yan Wentato et al. (2014) for the L4-L5 finite element model indicated a deformation value of 0.23mm, 0.47mm, 0.76mm, and 1.02mm under axial loads of 500 N, 1000N, 1500 N, and 2000 N, respectively [40]. This result shows a progressive increase in deformation with increasing compressive load, where the maximum direction deformation (1.03mm) in the current study closely aligns with the reported range under 1000N and 1500N axial loading in the literature. The minimum deformation found in the current study, which is (0.07mm at 126.196N), is also consistent with Yan Wentato et al. (2014), who reported 0.23mm at 500N, indicating a similar load-dependent stiffness response of the lumbar spine.

Similar to the findings of the current study, other research also demonstrates that compressive forces and posture significantly affect lumbar spine deformation. The study conducted by Sameer Pinjar et al. (2019) confirmed that as the load increases, the deformation in the lumbar spine region becomes more prominent, particularly in the lower lumbar segments (L3 - L5). This aligns with the present study, which observed significant deformation in these regions under higher compressive forces. Additionally, Sameer Pinjar et al. (2019) highlighted the risk of herniation and disc degeneration due to stress accumulation in lower lumbar spine, reinforcing the need to address lumbar health in lifting and ergonomic interventions [39].

Recent studies validate the findings of the current research on lumbar spine loading during lifting. Both Hambali Ariff et al. (2013) and Sameer Pinjar et al. (2019) reported that heavier weights and longer moment arms significantly increase compressive forces on the lumbar spine, aligning with the results in the current study showing the highest compressive loads under similar conditions [20,39]. Additionally Hambali Ariff et al. (2013) emphasized the critical impact of lifting techniques on spinal stress supporting the current study results that both moment arm length and lifting posture are crucial in managing lumbar spine loading [20].

Based on the current study findings, which indicate that compressive forces on the lumbar spine are significantly higher when lifting heavy objects at lower angle (more upright positions) and

decrease as the bending angle increases, targeted intervention can be developed to enhance workplace safety for construction laborers. The compressive stress observed on L5 vertebrae during lifting, especially under heavy loads, underscores the need for strategies to mitigate the impact of these factors on the lower back.

Given the findings of this study, it is recommended that Ethiopian construction laborers' work setups incorporate specific strategies to mitigate lumbar spine injuries. Employers should implement training programs that emphasize proper lifting techniques designed to reduce compressive force on the lumbar spine. Workers should be educated on maintaining a slight forward bend while lifting, as this can reduce the moment arm and, consequently, the compressive force on the lumbar spine. Emphasizing the importance of lifting from the legs rather than relying on the back muscles can also prevent excessive loading on the lumbar region. Training should highlight the risks associated with lifting in an upright posture with heavy loads for longer period, as the study shows this position places a significant compressive stress on the spine.

Furthermore, ergonomic interventions, such as providing mechanical lifting aids is essential in reducing the manual handling of heavy objects. These tools are particularly relevant in high-risk conditions where workers need to lift heavy items from lower angles, which the study identifies as contributing to increased spinal stress. Employers should also assess job tasks to minimize the need for manual lifting especially of heavy and awkwardly shaped objects. Incorporating rest breaks and rotation of tasks to prevent prolonged exposure to heavy lifting is crucial. As the current study reveals, exposure to high compressive force especially at L4-L5 region, increase the risk of long-term injury such as disc herniation.

Ultimately, the study highlights the importance of designing safe lifting protocols that reduce compressive forces on the lumbar spine. These protocols should be coupled with ergonomic equipment through worker training and a focus on minimizing risky posture to significantly reduce the incidence of lower back pain and spinal injuries among construction laborers.

Chapter Five
Conclusion and Recommendation

5.1 Conclusion

Lower back pain, a prevalent issue for construction laborers, is largely caused by manual material handling tasks such as heavy lifting, which affect the structure of the lower back. This study provided new insights into the biomechanical effects (in terms of stress and deformation responses on the lumbar spine) due to variation of the angle of force, length of moment arm and lifted weight. The research highlighted key biomechanical factors contributing to lower back injuries by performing a finite element analysis on the lumbar spine for a given compressive force. The findings offer important insight for improving workplace safety and developing recommendations for safer lifting practices to reduce injury risks among construction workers.

The calculation incorporated key variables such as weight lifted, angle (α) and length of moment arm across 210 distinct loading scenarios. A finite element model (FEM) of the lumbar spine was developed using Mimics, Geomagic Design X and ANSYS 19.0 software for accurate anatomical representation. After the model was finalized, the finite element analysis (FEA) was simulated using ANSYS 19.0 software to assess the stress distribution and biomechanical behaviors under various lifting conditions.

The results in the current study demonstrate that compressive force and Von Mises stress on the lumbar spine increase significantly with heavier loads, longer moment arms and improper lifting postures. In the current investigation, the maximum Von Mises stress values of 542.2 MPa, corresponding to a compressive load (F_{L1}) of 1419.71 N, was observed in the lumbar spine. This peak was obtained when lifting 125 kg load with angle (α) set at 0° and length of moment arm (lw) at 0.5 meter. Directional deformation values ranged from 0.0000629m to 0.001033m, with most significant deformation and stress affecting lower lumbar vertebrae during upright lifting. Compressive stress was reduced when angle (α) is set at 90° with a zero moment arm, as the bending position shifts the load distribution towards shear forces, which lessens the impact of compressive force on the lumbar spine.

The current research findings highlight that heavier loads and upright posture increase compressive force, particularly in the L4-L5 region, posing a higher risk of long-term injuries. To mitigate these risks, proper lifting techniques, ergonomic intervention and workplace safety protocols that reduce compressive stress on the lumbar spine should be implemented. Employers should implement training programs and mechanical lifting aids while promoting task rotation and rest breaks to minimize prolonged exposure to heavy lifting, ultimately reducing the incidence of lower back pain.

5.2 Recommendation

For future studies, it is recommended to explore the effects of shear forces during lifting tasks performed by construction laborers, as these forces also play significant role in spine stress and injury risk. Additionally, tracking the long-term effects of repeated lifting on the lumbar spine will provide valuable insights into cumulative damages and the development of chronic lower back issues. Investigating the impacts of different lifting techniques, including variation in load type (static Vs dynamics) and understanding of how individual variability affects spinal responses to loading, would enhance the understanding of safe lifting practices. Finally, identifying specific areas of the lumbar spine most impacted by these factors could lead to more targeted ergonomic interventions to reduce the incidence of lower back pain in physically demanding jobs.

References

[1] M.L.Ferreira et al., "Global, regional and national burden of low back pain, 1990-2020, its attributable risk factors, and projections to 2050: a systematic analysis of the Global Burden of Disease Study 2021," The Lancet Rheumatology, vol. 5, no. 6, pp. e316-e329, June, 2023, doi:10.1016/S2665-9913(23)00098-X.

[2] R. Op De Beeck, *Research on Work-related Low Back Disorders*. Luxemboug: European Agency for Safety and Health at work, 2000. ISBN 92-95007-02-6.

[3] L.D. Morris, K.J. Daniels, B. Ganguli, and Q.A. Louw, "An update on the prevalence of lower back pain in Africa: a systematic review and metaanalyses," BMC Musculoskeletal Disorder, vol. 19, no. 1, June, 2018, doi:10.1186/s1289-018-2075.

[4] M. Jengie and M. Afework, "Prevalence of self-reported work-related lower back pain and its associated factors in Ethiopia: a systematic review and meta- analysis," Journal of Environmental and Public Health, pp. 1-19, 2021, doi:10.115/2021/6633271.

[5] World Health Organization, "Occupational health." Feb. 2019. [Online] Available: http://www.who.int/health-topics/occupational-health. [Accessed: June 23, 2025].

[6] Health and Safety Executive, *Manual Handling Operations Regulations 1992*, 4th ed., Norwich, U.K.: Crown Copyright, 2016. ISBN 978-0-7276-6653-9.

[7] W. Thomas et al., "Estimating cost of care for patients with acute lower back pain: A retrospective review of patient records; family practice and neuromusculoskeletal medicine," *J. Am. Osteopath Assoc*., vol. 109, pp. 229-233, 2009, doi: 10.7556/jaoa.2009.109.4.229.

[8] S. Araujo, L. Carvalho, and E. Martins, "Lower back pain and level of disability among construction workers," *Fisioterapia em Movimento*, vol. 29, pp. 751-756, 2016, doi: 10.1590/1980-5918.029.004.ao11

[9] S. Saha & A. Roychowdlhury, " Application of finite element method in orthopedic implant design," Department of orthopedic surgery and Rehabilitation Medicine, *Journal of Long- Term Effects of Medical Implant* , Begell House, USA, pp. 55-82, 2009.

[10] "Ethiopia: Transforming construction industry," Stonenews, July 23, 2018. [Online]. Available:http://www.stonenews.eu/ethiopis-transforming-consturction-industry/. [Accessed: June 11,2025].

[11] M. Molla et al., "Occupational injuries among building construction workers in Gondar city," Department Environment and Occupational Health and safety, University of Gondar, Ethiopia, vol I, pp. 1-5, 2013.

[12] A. Qaseem, T. J. Wilt and M. A. Forciea, "Noninvasive treatment for acute, subacute and chronic lower back pain: A clinical practice guideline from the American College of Physicians," *Ann. Intern. Med*., vol. 166, no 7, pp 493-505, April. 2017, doi:10/7326/M16-236/M16-2367.

[13] G.E, Ehrlich, "Lower back pain," *World Health Organization*, vol. 81, no. 9, pp. 671-676, 2003.

[14] V.Theakston, "The Lumbar spine," *Teach Me Anatomy*, June 17,2020. [Online]. Available: http://teachmeanatomy.info/abdomen/bone/lumbar-spine/ [Accessed: July 1, 2025].

[15] D. K. Beasley, "Anatomy of the spine: Lumbar spine anatomy and pain" Mayfield Clinic, January, 20, 2020. [Online] Available: http://www.spine-health.com/. [Accessed: Nov. 23, 2025].

[16] M. Kurutz, "Finite element modeling of the human lumbar spine," Budapest University of Technology and Economics, Hungary, pp. 209-235, 2010.

[17] D. H. Cortes and D.M. Elliot, "The intervertebral disc: overview of disc mechanics," *The Intervertebral Disc Springer*, Vienna, June 8, 2013, doi: 10.1007/978-3-7091-1535-0-2.

[18] J.E. Muscolino, "Manual Therapy for the Low Back and Pelvis: A clinical Orthopedic Approach", 1st ed, St. Louis, Mo, USA: Elsevier, 2015. [Online Image]. Available: http://learnmuscles.com/product/manual-theraphy-for-the-low-back-and-pelvis-a-clincal-orthopeic-approach . [Accessed: Aug. 10, 2025].

[19] Cornell University Ergonomics Web, "Biomechanics of safe lifting," DEA 3250/6510 class notes. [Online] Available: https://www.ergo.human.cornell.edu/DEA3250Filpbook/DEA325notes/lifting.html#;:text=Lifiting%20Mechancis, load%20beng%20lifted%20or%20lowered. [Accessed: Jun. 2025].

[20] H. Ariff et al., "Finite Element Analysis of Conceptual Lumbar Spine for Different Lifting Position," World Applied Science Journal, Special Issue of Engineering and Technology, vol. 21, pp. 68- 75, 2013.

[21] H. Toda and H. Yamaoto, "Development of lower back load relief mechanism using principled of leverage for lifting a heavy object by hand," Department of Electric and Electronic Engineering, University of Toyama, vol. 6, pp. 1-5, 2016.

[22] S. Nurfaezah et al., "The effects of physiological biomechanical loading on intradiscal pressure and annulus stress in lumbar spine: A finite element analysis," *Journal of Applied Biomechanics*, Faculty of Mechanical Engineering, University Teknikal Malaysia Melaka, vol. I, pp. 1-9, 2017.

[23] X. Xiang et al., "Effect of parameters on Lumbar compressive Force during Patient Transfer," *Applied Science*, vol. 11, no. 24, pp. 11622, 2021, doi: 10.3390/app112411622.

[24] J.S.Han et al., “Loads in the spinal structures during lifting: Development of a three-dimensional comprehensive biomechanical model”, Department of orthopedics, West Virginia University, Morgantown, WV, USA, 2021.

[25] C. Zhang et al., “Biomechanical study of symmetric bending and lifting behavior in weightlifter with lumbar L4-L5 disc herniation and physiological straightening using finite element simulation,” *Bioengineering*, vol. 11, no. 8, pp. 825, August,2024, doi:10.3390/bioenbineering1108025.

[26] B.J. Devine, “Gentamicin therapy,” *Drug Intelligence Clinical Pharmacy*, vol. 8, pp. 605-655, 1974.

[27] A. Rohmann et al., “Comparison of the effects of bilateral posterior dynamic and rigid fixation device on the loads in the lumbar spine: A finite element analysis,” *European spine Journal*, vol. 16, no. 18, pp.1223-1231, 2007.

[28] “Ethiopia operation- Dangote Cement in Ethiopia,” Dangote Cement plc. [Online]. Available: https://www.dangotecement.com/ethiopia/. [Accessed: June 19, 2025].

[29] “River and M sand weight,” Mar. 10 2018. [Online]. Available: https://www.civilsir.com/what-is-m-sand-river-sand-m-sand-vs-river-sand/. [Accessed: May 21, 2025].

[30] A.K. Sengupta, “Biomechanics Lecture,” IE665 Applied Industrial Ergonomics, Department of Industrial Engineering, New Jersey Institute of Technology, NJ, USA, Lecture notes, 2004. [Online].Available: web.njit.edu/~sengupta /IE665/biomehcincs%20lecture.pdf. [Accessed: July 5, 2025].

[31] S.M. McGill, “The Biomechanics of Low Back Injury: Implications for Rehabilitation and injury prevention,” *Clinical Biomechanics*, vol. 12, no. 1, pp. 91-95, 1997.

[32] James A. Ashton Miller et al., “ Biomechanics of the human spine,” Biomechanics Research Laboratory, Department of Mechanical Engineering and Applied Mechanics, University of Michigan, *Basic orthopedics Biomechanics*, vol. II, Philadelphian, pp. 363-376, 1997.

[33] Materialise, “Materialise Mimics Medical version 21.0 -Release Notes,” Materialise, Jun. 2018. [Online] Avaliable: www.materialise.com. [Accessed: May,19,2025].

[34 J.K. Shin et al., “Stress and strain analyses of single and segmental Lumbar Spines based on accurate finite element model for vertebrae”, Biomedical Research Institute, pp s464-s471,2018 ISSN:0970-938X.

[35] J.L Wang et al., “Viscoelastic finite element analysis of a lumbar motion segment in combined compression and sagittal flexion,” Department of Orthopedics and Rehabilitation, USA, vol. 25, no. 3, pp. 310-318, 2000.

[36] H. Farajpour and N. Jamshidi,"Effect of different angles of the traction table on lumbar spine ligaments: a finite element study," Department of Biomedical Engineering, Unviersity of Isfahan, Iran, pp. 480- 481, 2017.

[37] X. Ming et al., "Lumbar spine finite element model for healthy subjects: development and validation," Computer Methods in Biomechanics and Biomedical Engineering, TX, USA, 2016, doi: 10/1080/1025582/2016.1193596.

[38] Y. H. Shash and R. H. Elden, "Computational analysis of L4-L5 inter spinous process devices and interbody fusion spacers using ceramic and polymeric materials via finite element modeling and artificial intelligence ," Sci. Rep.,vol. 15,pp 36142,2025. Doi:10.1038/s41598-025-20870-5.

[39] S. Pinjar et al., "Design and analysis of lumbar spine using finite element method," *International Research Journal of Engineering and Technology*, vol. 6, no. 6, pp. 3482- 3486, June, 2019.

[40] Y. Wentato et al., "Construction and analysis of a finite element model of human L4-L5 lumbar segment," *Chinese Journal of Biomedical Engineering*, vol. 33, no. 3, pp. 345- 350, June,2014.

Appendix I

Biomechanical Analysis Result

Weight of lifted object - M (Kg)	Length of moment arm from lifted weight - lw (m)	Angle made by the force of body weight with erector spinae muscle force - α	Erector Spinae muscle force - F_{muscle} (N)	Total Axial compressive Load - Fv (N)	Axial compressive Load in L1 - F_{L1} (N)
0	0	0	1147.24	1466.065	161.266
		30		1423.35	156.56
		45		1372.68	150.99
		60		1306.65	143.73
		90		1147.24	126.196
	0.1	0		1466.065	161.266
		30		1423.35	156.56
		45		1372.68	150.99
		60		1306.65	143.73
		90		1147.24	126.196
	0.2	0		1466.065	161.266
		30		1423.35	156.56
		45		1372.68	150.99
		60		1306.65	143.73
		90		1147.24	126.196
	0.3	0		1466.065	161.266
		30		1423.35	156.56
		45		1372.68	150.99
		60		1306.65	143.73
		90		1147.24	126.196
	0.4	0		1466.065	161.266
		30		1423.35	156.56
		45		1372.68	150.99
		60		1306.65	143.73
		90		1147.24	126.196
	0.5	0		1466.065	161.266
		30		1423.35	156.56
		45		1372.68	150.99
		60		1306.65	143.73
		90		1147.24	126.196
15		0	1147.24	1613.215	177.45
		30		1550.84	170.59

		45		1476.73	162.4403
		60		1446.25	159.0875
	0	90		1147.24	126.17
		0		1852.8	203.8
		30		1790.145	196.95
		45	1386.9	1715.98	188.75
		60		1619.88	178.187
	0.1	90		1386.9	152.55
		0		2103.635	231.39
		30		2041	224.53
		45	1637.66	1967.15	216.38
		60		1870.6	205.77
	0.2	90		1637.66	180.1426
		0		2348.87	258.37
		30		2286.5	251.515
		45	1882.9	2212.39	243.36
		60		2115.883	232.747
	0.3	90		1882.9	207.119
		0		2594.13	285.35
		30		2531.76	278.49
		45	2128.6	2457.65	270.34
		60		2361.43	259.72
	0.4	90		2128.6	234.146
		0		2834.63	311.8
		30		2772.2	304.942
		45		2697.74	296.75
		60		2601.643	286.18
	0.5	90	2368.6	2368.6	260.55
		0		1710.74	188.18
		30		1635.74	179.93
		45		1546.097	170.07
		60		1429.27	157.22
	0	90	1147.24	1147.24	126.196
		0		2114.6	232
25		30		2040.81	224.48
		45		1909.6	210.05
		60		1884.6295	207.309
	0.1	90	1551.8	1551.8	170.63
		0		2523.43	277.57
		30		2448.43	269.327
		45		2358.78	259.466

		60		2241.96	246.61
	0.2	90	1959.93	1959.93	215.59
		0		2932.1	322.53
		30		2857.1	314.28
		45		2767.457	304.42
		60		2650.655	291.57
	0.3	90	2368.6	2368.6	260.55
		0		3340.93	367.5
		30		3265.93	359.25
		45		3176.287	349.39
		60		3059.485	336.54
	0.4	90	2777.43	2777.43	305.517
		0		3749.5	412.45
		30		3675.18	404.26
		45		3584	394.46
		60		3468.718	381.55
	0.5	90	3186.8	3186.8	350.468
		0		1955.49	215.1039
		30		1848.13	203.29
		45		1719.51	189.146
		60		1551.902	170.7
	0	90	1147.24	1147.24	126.196
		0		2766.89	304.35
		30		2658.78	292.465
50		45		2529.7	278.26
		60		2362.55	259.8807
	0.1	90	1957.89	1957.89	215.36
		0		3586.18	394.47
		30		3478.32	382.61
		45		3349.7	368.467
		60	2777.43	3182.092	350.03
	0.2	90		2777.43	305.51
		0		4400.68	484.07
		30		4293.32	472.26
		45		4164.7	458.117
		60		3997.092	439.68
	0.3	90	3592.43	3592.43	395.1673
		0		5222.1	574.39
		30		5113.35	562.46
		45		4984.7	548.377
		60		4817.09	529.88

	0.4	90	4412.43	4412.43	485.36
		0		6033.55	663.68
		30		5925.89	651.847
		45		5796.86	637.65
		60		5629.662	619.26
	0.5	90	5225	5225	574.75
		0		2201.815	242.199
		30		2060.52	226.65
		45		1892.93	208.22
		60		1674.522	184.197
	0	90	1147.24	1147.24	126.196
		0		3420	376.3
		30		3279.88	360.7868
		45		3111.9	342.3
		60		2893.8825	318.327
	0.1	90	2366.6	2366.6	260.3
		0		4649.5	511.44
		30		4508.21	495
75		45		4340.2	477.4462
		60		4122.21	453.44
	0.2	90	3594.93	3594.93	395.44
		0		5875.75	646.33
		30		5734.46	630.79
		45		5567.53	612.427
		60		5348.46	588.33
	0.3	90	4821.183	4821.183	530
		0		7106.741	781.74
		30		6965.4	766.19
		45		6797.85	747.7
		60		6579.448	723.783
	0.4	90	6052.166	6052.166	665.73
		0		8325.6	915.816
		30		8184.88	900.3368
		45		8016.88	882.85
		60		7798.8825	857.877
	0.5	90	7271.6	7271.6	799.87
		0		2447.065	269.177
		30		2272.85	250.01
100		45		2066.35	227.29
		60		1797.15	197.68
	0	90	1147.24	1147.24	126.196

		0		4075.12	448.26
		30		3900.91	429.1001
		45		3694.411	406.38
		60		3425.2125	376.773
	0.1	90	2775.3	2775.3	305.28
		0		5717.48	628.92
		30		5543.27	609.75
		45		5336.77	587.044
		60		5067.57	557.43
	0.2	90	4417.66	4417.66	485.94
		0		8578.24	943.6
		30		8404.02	924.44
		45		8197.52	901.727
		60		7928.3	872.11
	0.3	90	7278.4	7278.4	800.624
		0		9049.991	995.499
		30		8812.77	969.4
		45		8606.276	946.69
		60		8337.07	917.07
	0.4	90	7687.166	7687.166	845.58
		0		10615.2	1167
		30		10441.01	1148.511
		45		10234.52	1125.79
		60		9965.312	1096.184
	0.5	90	9315.4	9315.4	1024.69
		0		2692.5	296.182
		30		2485.53	273.4
125		45		2239.94	246.39
		60		1899.9	208.98
	0	90	1147.24	1147.24	126.196
		0		5821.4	640.35
		30		5614.94	617.64
		45		5369.30	590.6285
		60		5029.16	553.207
	0.1	90	4276.65	4276.65	470.453
		0		6775.155	745.26
		30		6568.12	722.49
		45		6322.53	695.47
		60		5982.49	658.07
	0.2	90	5229.83	5229.83	575.28
		0		8818.9	970.07

		30		8611.87	947.3
		45		8366.28	920.29
		60		8026.24	882.88
	0.3	90	7273.58	7273.58	800.093
		0		10862.16	1194.837
		30		10655.62	1172.1182
		45		10410.03	1145.103
		60		10089.9625	1109.89
	0.4	90	9317.3	9317.3	1024.903
		0		12906.485	1,419.71
		30		12,699.45	1,396.94
		45		12,453.86	1,369.92
		60		12113.8225	1,332.52
	0.5	90	11361.18	11361.18	1,249.73

Appendix II

Finite Element Analysis Result

Weight of object lifted - M (Kg)	Length of moment arm from lifted weight - lw (m)	Angle made by the force of body weight with erector spinae muscle force - α	Axial compressive Load in L1 - F_{L1} (N)	Maximum Von Mises Stress (MPa)	Maximum Directional Deformation (m/m)
0	0	0	161.266	22.339	8.07E-05
		30	156.56	21.679	7.83E-05
		45	150.99	21.397	7.35E-05
		60	143.73	19.88	7.18E-05
		90	126.196	17.447	6.29E-05
	0.1	0	161.266	22.339	8.07E-05
		30	156.56	21.679	7.83E-05
		45	150.99	22.397	7.35E-05
		60	143.73	19.88	7.18E-05
		90	126.196	17.435	6.29E-05
	0.2	0	161.266	22.339	8.07E-05
		30	156.56	21.679	7.83E-05
		45	150.99	22.397	7.35E-05
		60	143.73	19.88	7.18E-05
		90	126.196	17.435	6.29E-05
	0.3	0	161.266	22.339	8.07E-05
		30	156.56	21.679	7.83E-05
		45	150.99	22.397	7.35E-05
		60	143.73	19.88	7.18E-05
		90	126.196	17.435	6.29E-05
	0.4	0	161.266	22.339	8.07E-05
		30	156.56	21.679	7.83E-05
		45	150.99	22.397	7.35E-05
		60	143.73	19.88	7.18E-05
		90	126.196	17.435	6.29E-05
	0.5	0	161.266	22.339	8.07E-05
		30	156.56	21.679	7.83E-05
		45	150.99	22.397	9.35E-05
		60	143.73	19.88	7.18E-05
		90	126.196	17.435	6.29E-05
15		0	177.45	24.611	8.90E-05
		30	170.59	23.56	8.52E-05
		45	162.4403	22.5	8.14E-05

		60	159.0875	22.033	7.96E-05
	0	90	126.17	17.435	6.29E-05
		0	203.8	28.32	1.03E-04
		30	196.95	27.2233	9.86E-05
		45	188.75	26.2	9.49E-05
		60	178.187	24.715	8.94E-05
	0.1	90	152.55	21.12	7.63E-05
		0	231.39	32.222	1.17E-04
		30	224.53	31.253	1.14E-04
		45	216.38	30.099	1.09E-04
		60	205.77	28.601	1.04E-04
	0.2	90	180.1426	24.99	9.04E-05
		0	258.37	35.29	1.22E-04
		30	251.515	34.968	1.28E-04
		45	243.36	33.923	1.24E-04
		60	232.747	32.311	1.17E-04
	0.3	90	207.119	29.03	1.05E-04
		0	285.35	39.913	1.46E-04
		30	278.49	38.93	1.42E-04
		45	270.34	37.6	1.37E-04
		60	259.72	36.215	1.32E-04
	0.4	90	234.146	32.615	1.19E-04
		0	311.8	43.596	1.60E-04
		30	304.942	42.724	1.57E-04
		45	296.75	41.4	1.52E-04
		60	286.18	40.032	1.46E-04
	0.5	90	260.55	36.29	1.32E-04
		0	188.18	26.2	9.49E-05
		30	179.93	24.87	9.03E-05
		45	170.07	23.56	8.52E-05
		60	157.22	22	7.95E-05
	0	90	126.196	17.435	6.29E-05
		0	232	32.311	1.17E-04
		30	224.48	31.253	1.14E-04
25		45	210.05	29.205	1.06E-04
		60	207.309	28.818	1.05E-04
	0.1	90	170.63	23.56	8.52E-05
		0	277.57	38.8	1.42E-04
		30	269.327	37.6	1.37E-04
		45	259.466	36.215	1.32E-04
		60	246.61	34.385	1.25E-04
	0.2	90	215.59	30.075	1.08E-04

		0	322.53	45.258	1.66E-04
		30	314.28	44.068	1.68E-04
		45	304.42	42.589	1.56E-04
		60	291.57	40.4	1.33E-04
	0.3	90	260.55	36.29	1.32E-04
		0	367.5	51.774	1.92E-04
		30	359.25	50.574	1.87E-04
		45	349.39	49.143	1.81E-04
		60	336.54	47.282	1.74E-04
	0.4	90	305.517	42.807	1.57E-04
		0	412.45	58.34	2.17E-04
		30	404.26	57.139	2.12E-04
		45	394.46	55.704	2.07E-04
		60	381.55	53.819	1.99E-04
	0.5	90	350.468	49.232	1.82E-04
		0	215.1039	29.904	1.09E-04
		30	203.29	28.32	1.03E-04
		45	189.146	26.257	9.51E-05
		60	170.7	23.56	8.52E-05
	0	90	126.196	17.435	6.29E-05
		0	304.35	42.589	1.56E-04
		30	292.465	40.933	1.50E-04
		45	278.26	38.86	1.42E-04
		60	259.8807	36.215	1.32E-04
	0.1	90	215.36	29.904	1.09E-04
		0	394.47	55.706	2.07E-04
		30	382.61	53.974	2.00E-04
		45	368.467	51.914	1.92E-04
50		60	350.03	49.23	1.81E-05
	0.2	90	305.51	42.689	1.56E-05
		0	484.07	68.935	2.52E-04
		30	472.26	67.177	2.52E-04
		45	458.117	65.075	2.44E-04
		60	439.68	62.348	2.33E-04
	0.3	90	395.1673	55.848	2.07E-04
		0	574.39	82.553	3.15E-04
		30	562.46	80.736	3.08E-04
		45	548.377	78.598	2.99E-04
		60	529.88	75.803	2.87E-04
	0.4	90	485.36	68.724	2.56E-04
		0	663.68	96.218	3.73E-04
		30	651.847	94.481	3.65E-04

		45	637.65	92.176	3.56E-04
		60	619.26	89.433	3.44E-04
	0.5	90	574.75	82.493	3.15E-04
		0	242.199	33.758	1.23E-04
		30	226.65	31.553	1.15E-04
		45	208.22	28.947	1.05E-04
		60	184.197	25.56	9.25E-05
	0	90	126.196	17.435	6.29E-05
		0	376.3	53	1.96E-04
		30	360.7868	50.798	1.88E-04
		45	342.3	48.072	1.77E-04
		60	318.327	44.651	1.64E-04
	0.1	90	260.3	36.29	1.32E-04
		0	511.44	73.029	2.76E-04
		30	495	70.567	2.66E-04
		45	477.4462	67.948	2.56E-04
		60	453.44	64.383	2.41E-04
	0.2	90	395.44	55.848	2.07E-04
75		0	646.33	93.623	3.62E-04
		30	630.79	91.214	3.52E-04
		45	612.427	88.38	3.40E-04
		60	588.33	84.682	3.24E-04
	0.3	90	530	75.821	2.88E-04
		0	781.74	131.18	4.55E-04
		30	766.19	125.28	4.44E-04
		45	747.7	118.51	4.30E-04
		60	723.783	110.12	4.41E-04
	0.4	90	665.73	97.218	3.73E-04
		0	915.816	189.32	5.55E-04
		30	900.3368	181.94	5.43E-04
		45	882.85	173.46	5.29E-04
		60	857.877	162.67	5.11E-04
	0.5	90	799.87	138.28	4.68E-04
		0	269.177	37.6	1.37E-04
		30	250.01	34.868	1.27E-04
		45	227.29	31.643	1.15E-04
		60	197.68	27.46	9.95E-05
100	0	90	126.196	17.435	6.29E-05
		0	448.26	63.578	2.38E-04
		30	429.1001	60.788	2.27E-04
		45	406.38	57.394	2.13E-04
		60	376.773	53.123	1.97E-04

	0.1	90	305.28	42.689	1.56E-04
		0	628.92	90.925	3.50E-04
		30	609.75	87.968	3.38E-04
		45	587.044	84.485	3.23E-04
		60	557.43	79.971	3.05E-04
	0.2	90	485.94	69.214	2.61E-04
		0	943.6	202.96	5.77E-04
		30	924.44	193.47	5.62E-04
		45	901.727	182.59	5.44E-04
		60	872.11	168.98	5.21E-04
	0.3	90	800.624	138.33	4.68E-04
		0	995.499	230.12	6.88E-04
		30	969.4	216.02	5.95E-04
		45	946.69	204.52	5.79E-04
		60	917.07	189.91	5.58E-04
	0.4	90	845.58	157.4	5.01E-04
		0	1167	340.68	7.69E-04
		30	1148.511	329.23	7.52E-04
		45	1125.79	314.74	7.31E-04
		60	1096.184	287.51	7.05E-04
	0.5	90	1024.69	246.316	6.43E-04
		0	296.182	41.46	1.52E-04
		30	273.4	38.203	1.40E-04
		45	246.39	34.353	1.25E-04
		60	208.98	29.054	1.05E-04
	0	90	126.196	17.435	6.29E-05
		0	640.35	92.695	3.58E-04
		30	617.64	89.183	3.43E-04
		45	590.6285	85.034	3.26E-04
		60	553.207	79.33	3.02E-04
	0.1	90	470.453	66.839	2.51E-04
125		0	745.26	117.6	4.29E-04
		30	722.49	109.68	4.13E-04
		45	695.47	101.3	3.95E-04
		60	658.07	95.45	3.70E-04
	0.2	90	575.28	82.688	3.16E-04
		0	970.07	216.55	5.98E-04
		30	947.3	204.83	5.80E-04
		45	920.29	191.45	5.58E-04
		60	882.88	173.5	5.29E-04
	0.3	90	800.093	138.33	4.68E-04
		0	1194.837	358.4	7.96E-04

		30	1172.1182	343.88	7.74E-04
		45	1145.103	327.03	7.49E-04
		60	1109.89	304.82	7.17E-04
	0.4	90	1024.903	246.316	6.43E-04
		0	1,419.71	542.2	1.03E-03
		30	1,396.94	519.34	1.01E-03
		45	1,369.92	497.5	9.76E-04
		60	1,332.52	467.89	9.36E-04
	0.5	90	1,249.73	399.73	8.50E-04

Appendix III

Mesh Convergence Test Result

Mesh Scenario	Mesh Element Size (mm)	Maximum Von Mises Stress (MPa)
Mesh 1	1	57.131
Mesh 2	2	44.93
Mesh 3	3	39.6
Mesh 4	4	39.19
Mesh 5	5	38.92
Mesh 6	6	38.85
Mesh 7	7	38.017
Mesh 8	8	37.23
Mesh 9	9	37.081
Mesh 10	10	37.06
Mesh 11	20	37.06
Mesh 12	30	37.06
Mesh 13	70	44.40
Mesh 14	100	50.30